Original Investigation

Endothelial Cell-Specific Molecule-1 Inhibits Albuminuria in Diabetic Mice

Xiaoyi Zheng [iD],[1] Lauren Higdon [iD],[1,2] Alexandre Gaudet,[1,3] Manav Shah [iD],[1] Angela Balistieri,[1] Catherine Li,[1] Patricia Nadai [iD],[3] Latha Palaniappan [iD],[4] Xiaoping Yang,[5] Briana Santo,[6] Brandon Ginley,[6] Xiaoxin X. Wang,[7] Komuraiah Myakala [iD],[7] Pratima Nallagatla,[8] Moshe Levi [iD],[7] Pinaki Sarder,[6] Avi Rosenberg [iD],[5] Jonathan S. Maltzman [iD],[1,2] Nathalie de Freitas Caires,[3,9] and Vivek Bhalla [iD][1]

Key Points

- Circulating endothelial cell-specific molecule-1 (Esm-1) inversely correlates with diabetic kidney disease.
- Addition of Esm-1 in susceptible mice reduces albuminuria, and deletion of Esm-1 in resistant mice mildly worsens albuminuria.
- Esm-1 attenuates podocyte injury and select IFN signaling, highlighting innate immunity as a potential mechanism of kidney disease.

Abstract

Background Diabetic kidney disease (DKD) is the most common cause of kidney failure in the world, and novel predictive biomarkers and molecular mechanisms of disease are needed. Endothelial cell-specific molecule-1 (Esm-1) is a secreted proteoglycan that attenuates inflammation. We previously identified that a glomerular deficiency of Esm-1 associates with more pronounced albuminuria and glomerular inflammation in DKD-susceptible relative to DKD-resistant mice, but its contribution to DKD remains unexplored.

Methods Using hydrodynamic tail-vein injection, we overexpress Esm-1 in DKD-susceptible DBA/2 mice and delete Esm-1 in DKD-resistant C57BL/6 mice to study the contribution of Esm-1 to DKD. We analyze clinical indices of DKD, leukocyte infiltration, podocytopenia, and extracellular matrix production. We also study transcriptomic changes to assess potential mechanisms of Esm-1 in glomeruli.

Results In DKD-susceptible mice, Esm-1 inversely correlates with albuminuria and glomerular leukocyte infiltration. We show that overexpression of Esm-1 reduces albuminuria and diabetes-induced podocyte injury, independent of changes in leukocyte infiltration. Using a complementary approach, we find that constitutive deletion of Esm-1 in DKD-resistant mice modestly increases the degree of diabetes-induced albuminuria versus wild-type controls. By glomerular RNAseq, we identify that Esm-1 attenuates expression of kidney disease–promoting and interferon (IFN)-related genes, including *Ackr2* and *Cxcl11*.

Conclusions We demonstrate that, in DKD-susceptible mice, Esm-1 protects against diabetes-induced albuminuria and podocytopathy, possibly through select IFN signaling. Companion studies in patients with diabetes suggest a role of Esm-1 in human DKD.

Introduction

Among complications of diabetes mellitus, kidney disease has the highest morbidity and mortality (1–3). The prevalence of diabetic kidney disease (DKD), defined as macroalbuminuria and/or impaired kidney function, is only 15%–30%, and few demographic or clinical features reliably predict which patients with diabetes (type 1 or type 2) will develop DKD (4–7).

[1]Division of Nephrology, Department of Medicine, Stanford University School of Medicine, Stanford, California
[2]Veterans Affairs Palo Alto Heath Care System, Palo Alto, California
[3]Institut National de la Santé et de la Recherche Médicale (INSERM), U1019-UMR9017-Center for Infection & Immunity of Lille, Pasteur Institute of Lille, University of Lille, Lille, France
[4]Division of Primary Care and Population Health, Stanford University School of Medicine, Stanford, California
[5]Division of Kidney-Urologic Pathology, Department of Pathology, Johns Hopkins University School of Medicine, Baltimore, Maryland
[6]Department of Pathology and Anatomical Sciences, University at Buffalo–The State University of New York, Buffalo, New York
[7]Department of Biochemistry, Molecular and Cellular Biology, Georgetown University Medical Center, Washington, DC
[8]Stanford Genome Center, Stanford University, Stanford, California
[9]Biothelis, Lille, France

Correspondence: Dr. Nathalie de Freitas Caires, Institut National de la Santé et de la Recherche Médicale (INSERM), U1019-UMR9017-Center for Infection & Immunity of Lille, Pasteur Institute of Lille, University of Lille, France, or Dr. Vivek Bhalla, Division of Nephrology, Department of Medicine, Stanford University School of Medicine, 780 Welch Rd., Stanford, CA 94305. Email: ndfreitascaires@biothelis.fr or vbhalla@stanford.edu

A better understanding of the molecular determinants of DKD could yield meaningful implications for human health.

Investigators of the Animal Models of Diabetic Complications Consortium have phenotypically characterized the clinical response to hyperglycemia among genetically distinct mouse strains (8, 9). One of these strains (DBA/2, DKD-susceptible) develops significant nephropathy compared with the more widely used strain (C57BL/6, DKD-resistant) (10). We previously compared glomerular transcriptome profiles from these two strains and, in DKD-susceptible mice, we found significantly higher expression of proinflammatory genes (11) and of genes related to endothelial dysfunction (12) and to immune-mediated vascular injury (13, 14). Among differentially regulated genes, we showed a glomerular-specific deficiency of endothelial cell-specific molecule-1 (Esm-1) in DKD-susceptible mice, and that Esm-1 acutely inhibits leukocyte infiltration (11, 15).

Esm-1 is a glomerular-enriched, secreted glycoprotein with putative functions in inflammation and developing vasculature, although its effects on the kidney are unknown. Esm-1 transcription is modulated by proinflammatory cytokines, including interferon(IFN)-γ (16). One putative function of Esm-1 is to inhibit the interaction of lymphocyte function-associated antigen-1 (LFA-1) with intercellular adhesion molecule-1 (ICAM-1) (15, 17), a well-recognized step of leukocyte infiltration. During development, Esm-1, regulated by vascular endothelial growth factor, is also expressed in tip cells at the leading edge of vascular outgrowths (18). In samples from healthy volunteers, we showed that Esm-1 is enriched in kidney compared with other tissues and, within the kidney, is highest in glomeruli (11). However, this glomerular-enriched Esm-1 is relatively deficient in patients with DKD versus healthy volunteers (11, 19, 20). We and others have shown that Esm-1 reduces leukocyte transmigration *in vitro* (11, 15), and Esm-1 glomerular mRNA and protein are decreased in DKD-susceptible versus DKD-resistant mice and demonstrate an attenuated increase with hyperglycemia (11). Whether circulating Esm-1 ameliorates DKD has not been previously studied.

We hypothesize that Esm-1 deficiency contributes to kidney injury in DKD-susceptible mice. Further, we posit that addition of Esm-1 in DKD-susceptible mice would attenuate kidney injury, and Esm-1 deletion in DKD-resistant mice would promote kidney injury. In this study, using complementary approaches, we determine the *in vivo* contribution of Esm-1 to albuminuria and glomerular and/or tubulointerstitial inflammation in murine DKD and analyze the histologic and transcriptomic response to Esm-1 rescue in DKD-susceptible mice. We also explore the association between circulating Esm-1 and albuminuria in patients with DKD.

Materials and Methods
Induction of Diabetes
We injected 8-week-old male DKD-susceptible (DBA/2J) or DKD-resistant (C57BL/6J) mice (Jackson Laboratories, Bay Harbor, ME) intraperitoneally with 40 mg/kg body wt of streptozotocin (STZ; Sigma-Aldrich, St. Louis, MO) versus vehicle (sodium citrate [pH 4.5]) daily for five consecutive days. We then supplemented mice with 10% sucrose water to prevent hypoglycemia. Four weeks after the injection, we fed diabetic mice with a high-fat diet (Research Diets, New Brunswick, NJ) for five additional weeks until euthanasia (21, 22). We measured body weight once per week. We quantified fasting blood glucose with a Bayer Contour glucometer at 4 weeks post-STZ injection to verify hyperglycemia. We collected urine samples at 9 weeks post-STZ injection and euthanized mice at 10 weeks post-STZ injection. We prepared plasma samples from retro-orbital blood and stored them at $-80°C$. We then prepared glomerular and tubulointerstitial single cells for flow cytometry analysis.

Quantification of Albuminuria
We collected urine from mice, singly housed in metabolic cages (Tecniplast, Buguggiate, Italy). We quantified urine albumin by ELISA and creatinine by a Creatinine Companion kit (Exocell, Philadelphia, PA), following the manufacturer's instructions. For quantification of albumin, we diluted urine samples at 1:10 to 1:15 for vehicle-treated mice and at 1:100 to 1:300 for polyuric, diabetic mice. For quantification of creatinine, we diluted urine samples 1:13 for vehicle-treated mice.

Single-Cell Preparation of Glomerular and Tubulointerstitial Tissue
We anesthetized mice with isoflurane and euthanized them after cardiac perfusion. We isolated mice kidneys and dissociated tissue by forceps, and then by gentleMACS tissue homogenizer with the program h_cord 01.01 (Miltenyi Biotec, San Diego, CA) in 5-ml Hepes Ringer buffer (118-mM sodium chloride, 17-mM H-Hepes, 16-mM Na-Hepes, 14-mM glucose, 3.2-mM potassium chloride, 2.5-mM calcium chloride dihydrate, 1.8-mM magnesium sulfate heptahydrate, 1.8-mM potassium dihydrogen phosphate). After centrifugation ($200\times g$ for 10 minutes), we resuspended the kidney tissue in Hepes Ringer buffer containing 0.2% collagenase I (Worthington Biochemical, Lakewood, NJ) and 0.2% hyaluronidase (Sigma-Aldrich), 90 ml/g kidney weight, and rotated at 37°C for 2 hours. We washed the digested tissue multiple times with Hepes Ringer and centrifuged at $259\times g$ for 2 minutes, until the supernatant became clear. We resuspended the tissue in 13 ml Hepes Ringer buffer and passed tissue through a 40-μm cell strainer (Corning, Corning, NY) twice and a 100-μm strainer (Thermo Fisher Scientific, Waltham, MA) once to isolate glomeruli. The flow through from the 40-μm strainer contained tubulointerstitial cells. The flow through from the 100-μm strainer contained glomeruli. We centrifuged both glomerular and tubulointerstitial fractions at 4000 rpm for 10 minutes. We resuspended the tubulointerstitial single cells with 1 ml 4% neutral buffered formalin (Thermo Fisher Scientific) and fixed for 20 minutes at room temperature, then stored in PEB buffer (1× PBS, 2 mM EDTA, 0.5% BSA) at 4°C. We resuspended the glomerular fraction in 1 ml HBSS buffer with calcium and magnesium ions (Hyclone, Logan, UT) containing 0.1–0.2 mg/ml Liberase Research Grade (Roche, Mannheim, Germany), and incubated glomeruli in 24-well tissue culture plates at 37°C for 24 hours. The next day, we broke the glomeruli by pipetting up and down 10 times and then centrifuged the

glomerular single cells at 8000 rpm for 10 minutes, fixed cells with 4% neutral buffered formalin (Thermo Fisher Scientific) for 20 minutes at room temperature, and then stored cells in PEB buffer at 4°C.

Flow Cytometry

We permeabilized formalin-fixed glomerular and tubulointerstitial single cells with 0.25% Tween-20 in PEB buffer at room temperature for 30 minutes and blocked cells with Fc Block (clone 2.4G2; BD Biosciences, San Jose, CA) diluted in 0.25% Tween-20 on ice for 10 minutes. We stained cells with fluorescent-conjugated antibodies (Supplemental Table 1) on ice for 30 minutes. After washing, we resuspended cells in 200 μl PEB buffer for flow cytometry analysis on a Scanford Flow Cytometer in the Stanford Shared FACS Facility. We used Flowjo 10 software (Becton Dickinson, Ashland, OR) to analyze data. For CD45(+) cells, we classified CD68(+)Ly6G(−) cells as macrophages, CD68(−)Ly6G(+) cells as neutrophils, and CD68(−)Ly6G(−) cells as others (likely lymphocytes).

Esm-1 ELISA

We quantified human serum Esm-1 by ELISA (Lunginnov, Lille, France) and mouse plasma Esm-1 by ELISA (Aviscera Biosciences, Santa Clara, CA), following the manufacturer's instructions.

Hydrodynamic Injection to Overexpress Circulating Esm-1

Dr. Justin Annes (Stanford University) kindly provided pT3-hEsm-1-V5 and pT3-GLuc (*Gaussia* Luciferase). The Emory University Integrated Genomics Core facility (Atlanta, GA) subcloned mouse or human Esm-1 cDNA from pCMV6 (Origene, Rockville, MD) into pT3. We prepared plasmids using an EndoFree Plasmid Maxi Kit (Qiagen, Germantown, MD). One week before the induction of diabetes, we performed hydrodynamic injection to overexpress Esm-1. We diluted three plasmids: pT3-mEsm-1-V5 (25 μg), pT3-GLuc (25 μg), and pCMV(CAT)T7-SB100 Sleeping Beauty transposase (2.5 μg; Addgene, Cambridge, MA) (23) in endotoxin-free saline (Teknova, Hollister, CA). We injected the plasmid solution through the mouse tail vein at 0.1 ml/g body weight with a 27G needle in 6–8 seconds. Saline injection serves as the negative control. At the time of euthanasia, we collected retro-orbital blood, prepared plasma samples, and quantified Esm-1 and luciferase activity. To validate the uptake of plasmids by hepatocytes, we performed hydrodynamic injection to express green fluorescent protein. We then euthanized these mice and verified green fluorescence protein expression using a Leica DM5000 (Leica, South San Francisco, CA).

Gaussia Luciferase Assay

We quantified plasma luciferase activity by a BioLux *Gaussia* Luciferase Assay Kit (NEB, Ipswich, MA) from 10 μl plasma acquired by retro-orbital bleeding, following the manufacturer's instructions.

Generation of Esm-1 Knockout Mice

We inserted loxP recognition sites to flank exons 1 and 2 of the mouse Esm-1 gene (Ensembl identifier ENSMUSG00000042379). In collaboration with the Institut Clinique de la Souris (Strasbourg, France), we transfected a targeting cDNA fragment containing a neomycin resistance cassette surrounded by loxP sites into mouse embryonic stem cells by electroporation, allowing replacement of exons 1 and 2 of Esm-1 by the neomycin resistance cassette through homologous recombination. After transfection, we selected embryonic stem cells for recombination of Esm-1 with G418-containing medium, validated these clones by Southern blot, and injected clones into blastocysts and then into pseudopregnant female mice. We then crossbred the offspring to generate mice that lack Esm-1 exons 1 and 2 on homologous chromosomes. We then crossbred these mice with Cre deleter mice to remove the neomycin resistant cassette. For genotyping, we extracted genomic DNA from mouse tails and performed PCR with the REDExtract-N-Amp Tissue PCR Kit (Sigma-Aldrich) following the manufacturer's instructions and analyzed samples on agarose gel. We used 1f and 1r primer pairs to generate a 310-bp fragment for the wild-type allele, and 1f and 2r primer pairs to generate a 442-bp fragment, indicative of the knockout allele. Primer sequences are in Supplemental Table 2.

Podocyte Staining

We stained 3- and 9-μm paraffin kidney sections with anti–WT-1 antibody (ab15249; Abcam, Cambridge, MA) according to published protocols (24). Briefly, we performed antigen retrieval on rehydrated sections in sodium citrate buffer, pH 6.0, at 95°C for 1 hour. After blocking with 20% goat serum, we incubated sections with 1:400 diluted anti–WT-1 antibody at 4°C overnight. We then blocked sections with a Biotin/Avidin blocking kit, incubated with biotinylated goat anti-rabbit secondary antibody, and developed with ABC and DAB kits (Vector Lab, Burlingame, CA). We further stained sections with Periodic acid–Schiff reagent (Sigma-Aldrich), without hematoxylin counterstain. After dehydration, we mounted sections with EUKITT mounting medium (Thermo Fisher Scientific). We captured images of stained sections with the Nanozoomer Digital Scanner (Stanford Canary Center Imaging Core Facility). We then exported images containing 50 glomeruli per mouse and analyzed with machine learning tools developed using the Cord online platform (https://app.cord.tech/login). We used approximately 40 images to train models to initiate the recognition of glomerular tuft area. We used a confidence of 0.4 to recognize podocytes and 0.6 to recognize the glomerular tuft area. We then quantified podocyte per glomerular volume according to the Animal Models of Diabetic Complications Consortium protocol.

RNA Sequencing

We extracted kidney glomeruli from control mice, diabetic mice, and diabetic mice with overexpression of mouse Esm-1. We isolated glomerular RNA using the Zymo Research RNA preparation micro kit (Zymo Research, Irvine, CA). We removed genomic DNA using RNase-free DNase I (Fermentas, Waltham, MA). We then reversed transcribed RNA into cDNA by using Improm II reverse transcriptase (Promega, Madison, WI) and random hexamer primers (Genelink, Elmsford, NY). We submitted cDNA samples to CD Genomics (New York, NY) for DNA

quality control, library preparation, and sequencing (Illumina Novaseq PE150 sequencing, 20M read pairs).

We then trimmed raw paired-end FASTQ files using Trimmomatic version 0.36. We performed RNA-sequencing (RNAseq) alignment to the reference mm9 using STAR version 2.5.3a and default conditions. We filtered gene counts for low expressing genes and performed differential expression analyses using the DESeq2 version 1.28.1 R package installed in R version 4.0.2, with default settings. We submitted the data to Geobank with the accession number GSE175449.

Quantitative RT-PCR

We prepared cDNA as described above. We then used Fast Syber Green Master Mix (Applied Biosystems, Foster City, CA) to quantify cDNA samples (1:5 to 1:25 diluted) with the primers listed in Supplemental Table 3 at a melting temperature of 60°C. We used the StepOne PCR machine (Applied Biosystems) provided by the Stanford Protein and Nucleic Acid (PAN) Facility.

Biorepository

We collected serum samples from patients in two separate cohorts: (1) patients who self-identified with diabetes mellitus at the Palo Alto Medical Foundation from 2011 to 2012 ($N=250$), and (2) patients who were consented for the Stanford Precision Biobank regardless of status of diabetes mellitus or kidney disease ($N=2579$). From these cohorts, we extracted data from the electronic health record and maintained a deidentified, secure database. We verified patients with type 2 diabetes using physician-recorded diagnosis (International Classification of Diseases, Ninth Edition codes 250.X0, 250.X2), abnormal laboratory values according to American Diabetes Association guidelines (two of any hemoglobin A1c ≥6.5%, fasting blood glucose ≥126 mg/dl, random blood glucose ≥200 mg/dl, or oral glucose tolerance test ≥200 mg/dl) (25), or use of any antidiabetic medications. Among patients with at least one recorded urine albumin or protein and one serum creatinine measurement ($N=143$ samples), after verification of diabetes mellitus, we classified these patients with (1) normoalbuminuria (<30-mg urine albumin per gram of creatinine), (2) microalbuminuria (30–300-mg urine albumin per gram of creatinine), or (3) macroalbuminuria (≥300-mg urine albumin per gram of creatinine). We retained patients in the cohort with a stable classification of albuminuria within the months immediately preceding and after the biospecimen collection date. In total, we studied 99 patients with sufficient and stable baseline characteristics. Among patients with normo- or microalbuminuria with a baseline eGFR ≥30 ml/min per 1.73 m^2 using the Chronic Kidney Disease Epidemiology Collaboration equation (26), we classified patients as progressors if longitudinal data showed a persistent transition from normo- to micro- or macroalbuminuria, or micro- to macroalbuminuria. The median (interquartile range) time between baseline urine measurement and serum sample collection was 6 (13.5) months, and follow-up data was available for 1.75 (3.0) years. Years of available follow-up data did not significantly differ between groups. We processed samples by centrifugation and stored aliquots at −80°C.

Study Approval

The Palo Alto Medical Foundation Institutional Review Board (IRB) approved the collection and storage of human samples and deidentified clinical data. The Stanford University School of Medicine IRB approved the collection and storage of human samples and deidentified clinical data from the Stanford Precision Biobank. The Stanford Research Compliance Office Administrative Panel for the Protection of Human Subjects–IRB approved the use of stored human sera. The Stanford Institutional Animal Care and Use Committee approved the experiments in mice. The animal protocol adheres to the National Institutes of Health (NIH) Guide for the Care and Use of Laboratory Animals.

Statistical Analyses

For statistical comparisons with normal data distribution, we used the unpaired t test as appropriate for two columns, parametric one-way ANOVA as appropriate for more than two columns, and two-way ANOVA for grouped tables. We used Bonferroni correction to adjust for multiple comparisons, as indicated, and used Dunnett T3 correction in one-way ANOVA assuming different SDs. For non-normal data distribution, we used the Mann–Whitney test for two columns, and the Kruskal–Wallis test for more than two columns. For inference testing, we examined log urinary albumin-creatinine ratio to accommodate model assumptions. For podometrics, we analyzed data using Minitab Statistical Software version 19 (Minitab 17 Statistical Software [2010]; Minitab, State College, PA). We assessed differences between two groups with the unpaired, two-sample t test. We adjusted by Welch correction for unequal variances when necessary. For RNAseq analysis, we compared DESeq2-normalized, log-transformed gene counts (log2[normalized counts+]) for comparisons, as indicated, and used the q-value function from the q-value R package with default settings to run adjustment for multiple comparisons. We used the online software Metascape (http://metascape.org/) tool to perform Gene Ontology analysis (27) using genes with q-values <0.05 as inputs. We ran this analysis with default parameters to infer a hierarchic clusterization of significant ontology terms into a tree on the basis of κ-statistical similarities among gene memberships. We selected the term with the best q-value within each cluster as its representative term. We retained ontology clusters with a q-value of <0.05 as significantly enriched. In analyses restricted to specific gene sets, we generated q-values to run adjustment for multiple comparisons as indicated. We designated statistical significance at a two-sided P value of <0.05 for all biologically meaningful comparisons. For each experiment, we note the number of samples in the corresponding figure legend. We represent data per mouse when indicated and include mean±SEM.

Results

Circulating Esm-1 Inversely Correlates with Albuminuria and Glomerular Leukocyte Infiltration in Mice with DKD

We induced diabetes in DKD-susceptible mice, as indicated in Figure 1A. Compared with nondiabetic controls, diabetic DKD-susceptible mice show similar plasma Esm-1 concentrations, and significantly higher albuminuria
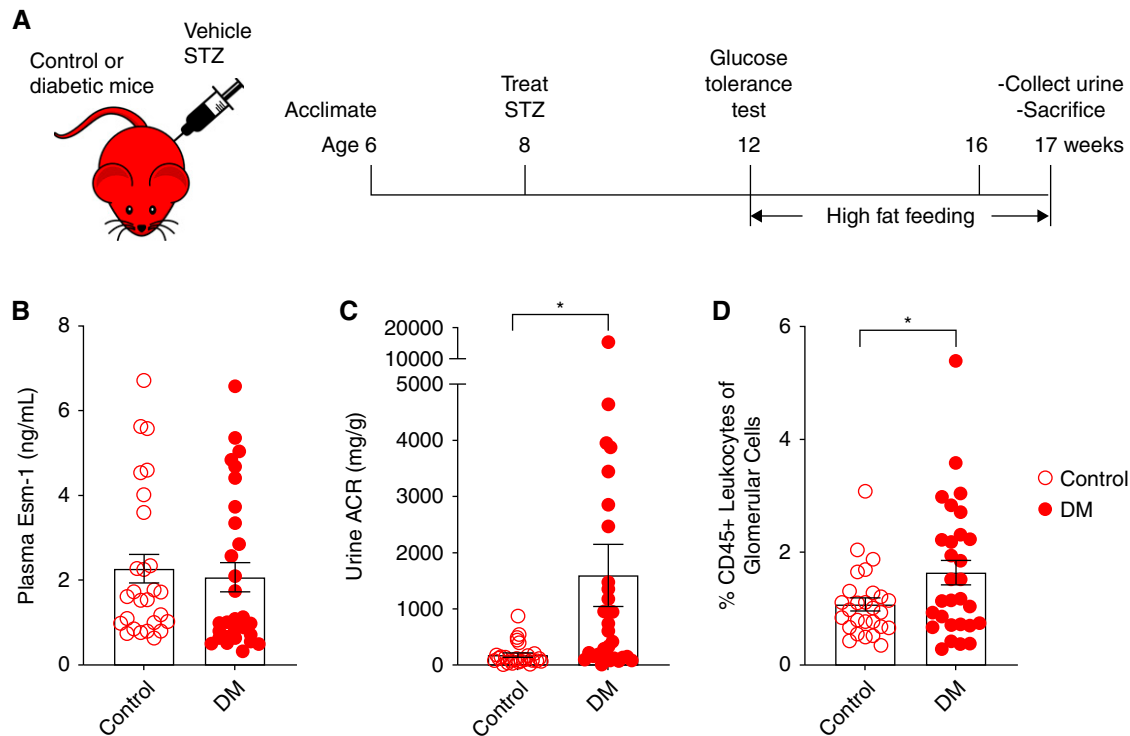
Figure 1. | **Plasma Esm-1, albuminuria, and glomerular leukocytes vary in DKD–susceptible mice.** (A) Timeline of experimental design. We treated mice with vehicle versus STZ and high-fat feeding, followed by euthanasia at 17 weeks of age. We quantified (B) plasma Esm-1, (C) urine albumin-creatinine ratio (ACR), and (D) glomerular leukocytes. Open circles, control mice; closed circles, diabetic (DM) mice. Results are presented per mouse and include mean±SEM. R^2 for nonlinear regression (solid line) is shown. $n=27–29$ per group. *$P<0.05$ versus control mice by unpaired t test.

(Figure 1, B and C). We quantified mouse kidney leukocyte infiltration in both glomeruli and tubulointerstitium (Supplemental Figure 1A). We show that 1.1%±0.1% and 2.8%±0.7% of cells are CD45(+)-positive leukocytes in healthy mice glomeruli and tubulointerstitium ($n=29–30$ mice per group), respectively, and the predominant leukocyte subtype are macrophages (Supplemental Figure 1, B and C). Diabetic mice have more pronounced glomerular infiltration compared with control mice (Figure 1D). However, on the basis of the wide range of albuminuria and leukocyte infiltration in diabetic mice, we next compared the association of plasma Esm-1 concentration with albuminuria and glomerular leukocytes. Albuminuria inversely correlates with plasma Esm-1 concentration ($R^2=0.77$) with an inflection at plasma Esm-1 of approximately 3 ng/ml (Figure 2A). Diabetic mice with low plasma Esm-1 (<3 ng/ml) have significantly higher albuminuria compared with nondiabetic controls, whereas diabetic mice with higher plasma Esm-1 have no change in albuminuria (Figure 2B). Plasma Esm-1 also inversely correlates with levels of glomerular leukocyte infiltration ($R^2=0.49$) and, for mice with plasma Esm-1 >3 ng/ml, diabetes has virtually no effect on leukocyte infiltration (Figure 2, C and D). To assess causality, we used overexpression and knockout of Esm-1.

Hydrodynamic Injection Stably Increases Circulating Esm-1 in Mice

Intraperitoneally injected Esm-1 protein only transiently increases plasma Esm-1 (Supplemental Figure 2, Supplemental Appendix 1). Therefore, we used hydrodynamic tail-vein injection for stable overexpression and secretion of Esm-1 into the systemic circulation (Supplemental Figure 3, A and B) (28). Plasma luciferase significantly increases and correlates with plasma Esm-1 1 week after coinjection (Supplemental Figure 3C).

Mouse and Human Esm-1 Decrease the Degree of Albuminuria in Diabetic Mice, Independent of Leukocyte Infiltration

We performed hydrodynamic injection of a mouse or human Esm-1–expressing plasmid 1 week before the induction of diabetes (Figure 3A). Hydrodynamic injection in diabetic mice significantly increases circulating plasma Esm-1 approximately ten-fold (mouse: 1.3±0.2 versus 12.7±1.5 ng/ml, $P<0.001$, $n=10–13$ mice per group; human: 0.03±0.03 versus 5.61±1.41 ng/ml, $P=0.02$, $n=8–11$ mice per group; Figure 3, B and C). Overexpression of mouse Esm-1 does not appreciably alter the incidence of hyperglycemia or alter body weight (Figure 3, D and E). Esm-1 attenuates the induction of albuminuria in diabetic mice (mouse: 220.2±42.2 versus 1193.1±396.3 mg/g, $P=0.54$; $n=10–15$ mice per group; human: 103.0±23.4 versus 118.0±57.3 mg/g, $P>0.99$, $n=6–8$ mice per group) compared with saline-injected controls (180.1±43.5 versus 2028.1±676.9 mg/g, $P=0.002$, $n=23–24$ mice per group; Figure 3F). Overexpression of mouse, but not human, Esm-1 significantly reduces total glomerular leukocytes (Figure 3G) but not tubulointerstitial leukocytes or specific
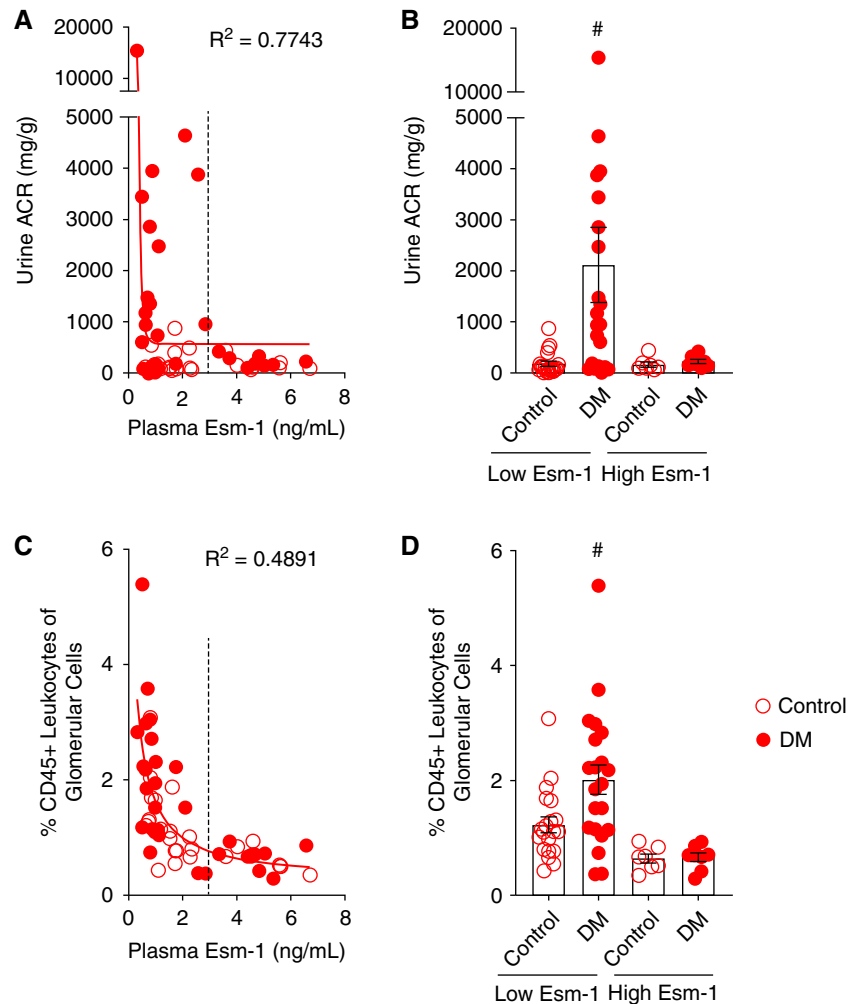
Figure 2. | Esm-1 inversely correlates with albuminuria in diabetic, DKD-susceptible mice. (A) We correlated urine albumin-creatinine ratio (ACR; n=27–29 mice per group) and (C) glomerular leukocytes (n=27–29 mice per group) with plasma Esm-1. Dotted lines represent plasma Esm-1 of 3 ng/ml. We quantified (B) urine ACR and (D) glomerular leukocytes in control and diabetic mice, segregated by low or high Esm-1 groups. Low Esm-1 refers to plasma Esm-1 <3 ng/ml. Open circles, control mice; closed circles, diabetic (DM) mice. Results are presented per mouse and include mean±SEM. R^2 for nonlinear regression (solid line) is shown. #P<0.05 versus control mice by unpaired t test.

leukocyte subsets in either kidney compartment (Supplemental Figure 4). Moreover, albuminuria and glomerular leukocytes do not correlate in this model (Supplemental Figure 5). Taken together, overexpression of Esm-1 reduces albuminuria, and the glomerular response is consistent across species.

Esm-1 Deletion in DKD-Resistant Mice Modestly Increases Albuminuria, Independent of Leukocyte Infiltration

As a complementary approach, we engineered and validated a constitutive knockout of Esm-1 on a DKD-resistant background (Supplemental Figure 6). Knockout mice have no detectable circulating plasma Esm-1 and, with induction of diabetes, have similar fasting blood glucose and body weight compared with DKD-resistant wild-type littermate controls (Figure 4, A–D). The degree of diabetes-induced albuminuria is modestly, but significantly, higher in Esm-1 knockout mice (50.6±14.6 versus 296.8±65.8 mg/g, P=0.001, n=8–11 mice per group) compared with DKD-resistant,

wild-type littermate controls (38.1±8.8 versus 207.0±100.5 mg/g, P=0.06, n=6–9 mice per group; Figure 4E). In contrast to the effects on albuminuria, Esm-1 knockout mice do not exhibit diabetes-induced glomerular leukocyte infiltration (Figure 4F). In fact, glomerular leukocytes (macrophages) are modestly decreased in knockout mice in diabetics versus controls. Tubulointerstitial leukocytes or leukocyte subsets are not appreciably different in knockout mice or wild-type littermate controls (Supplemental Figure 7).

Esm-1 Attenuates WT-1(+) Podocyte Injury

In histologic analysis, using WT-1 as a marker of both parietal and visceral podocytes (29,30) (Supplemental Figure 8, Supplemental Appendices 1 and 2), diabetes significantly decreases the number of WT-1(+) podocytes (Figure 5A), and addition of mouse Esm-1 prevents this podocyte loss (Figure 5B). Using p57 as a marker primarily of visceral podocytes, diabetes modestly increases the number of p57(+) podocytes with larger area (Supplemental
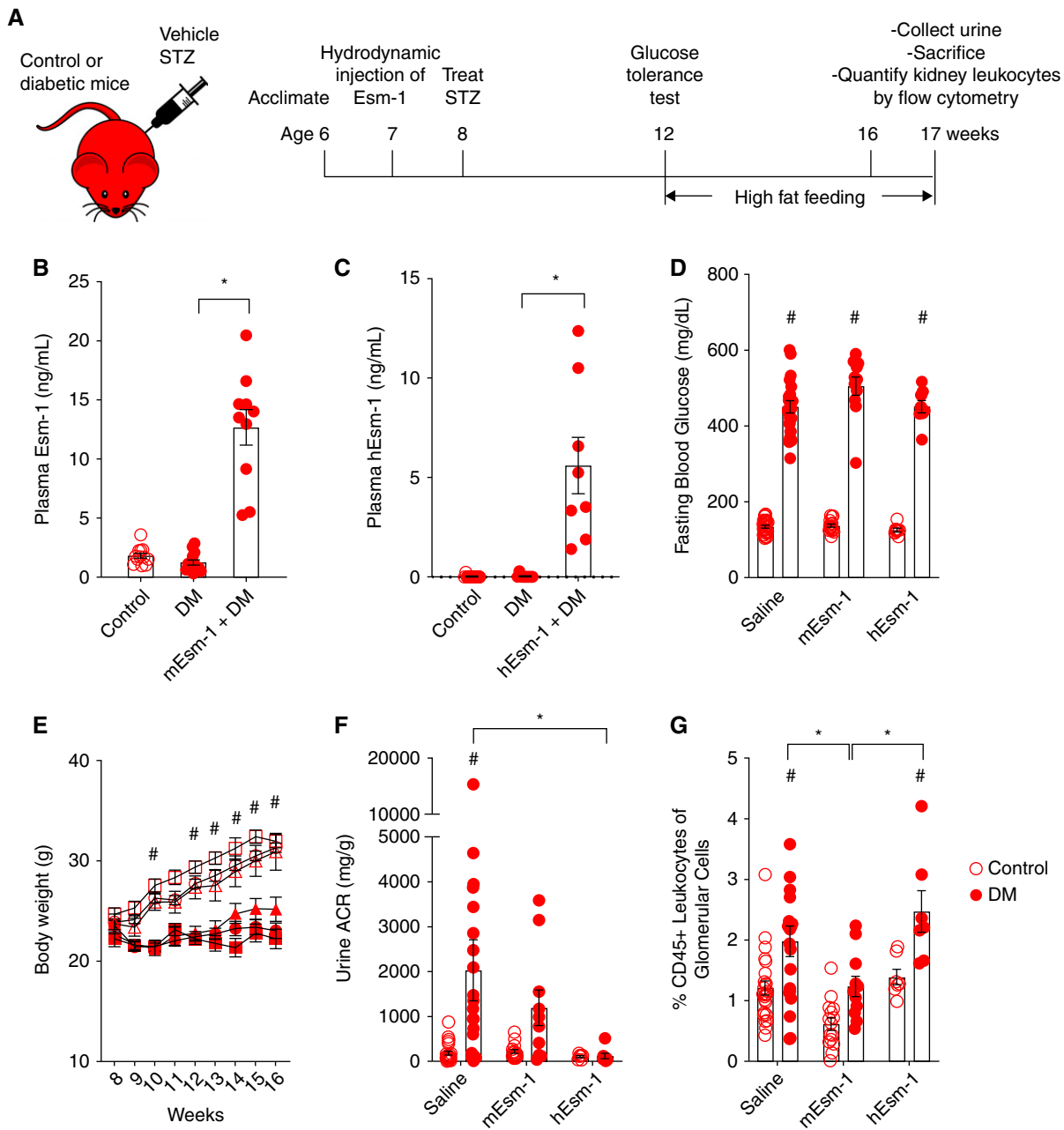
Figure 3. | Systemic overexpression of Esm-1 reduces diabetes-induced albuminuria in DKD-susceptible mice. (A) Timeline of experimental design. We induced expression of mouse (m) or human (h) Esm-1 by hydrodynamic injection and treated mice with vehicle versus STZ and high-fat feeding at indicated time points, followed by euthanasia at 17 weeks of age. We quantified (B) mouse and (C) human plasma Esm-1, (D) fasting blood glucose, (E) body weight, (F) urine albumin-creatinine ratio (ACR), and (G) glomerular leukocytes in control and diabetic mice. $n=8–13$ mice per group in (B) and (C); $n=6–24$ mice per group in (D–G). Open circles, control mice; closed circles, diabetic (DM) mice. In all panels except (E), results are presented per mouse and include mean±SEM. In (E), values for mice with overexpression of mouse Esm-1 are shown as squares and with overexpression of human Esm-1 are shown as triangles. Results are presented as mean±SEM. *$P<0.05$ compared across groups as indicated, #$P<0.05$ versus control mice, by one-way ANOVA (B–C) or two-way ANOVA (D–G).

Figure 9B) and glomerular podocyte coverage ($P=0.006$; Supplemental Figure 9C), which are markers of podocyte hypertrophy/injury (29, 31) (Supplemental Appendices 1 and 2). Overexpression of mouse Esm-1 reduces the number of p57(+) podocytes with larger area (Supplemental Figure 9B) and glomerular p57(+) podocyte coverage compared with diabetes alone ($P<0.001$; Supplemental Figure

9C, Supplemental Table 4). In contrast to WT-1, we find that the total number of p57(+) podocytes do not decrease at this stage of diabetes (Supplemental Figure 9, D and E). Diabetes increases the fractional glomerular area of fibronectin and collagen type IV, which are sensitive markers of mesangial matrix expansion (32); however, overexpression of Esm-1 does not significantly reduce expression of these
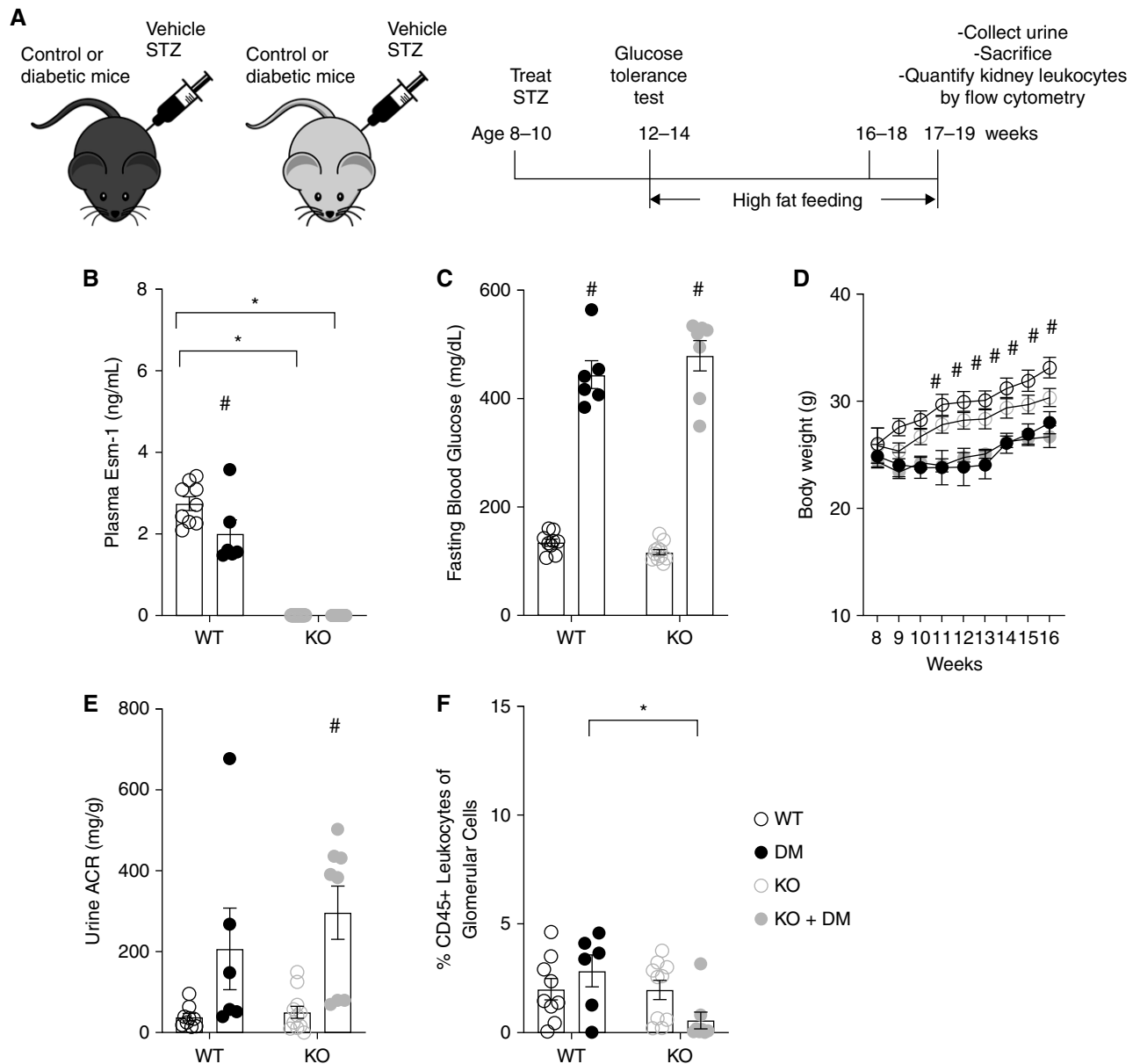
Figure 4. | Constitutive deletion of Esm-1 induces albuminuria in diabetic DKD-resistant mice. (A) Timeline of experimental design. We treated wild-type and Esm-1 knockout mice with vehicle versus STZ and high-fat feeding, followed by euthanasia at 17–19 weeks of age. We quantified (B) plasma Esm-1, (C) fasting blood glucose, (D) body weight, (E) urine albumin-creatinine ratio (ACR), and (F) glomerular leukocytes in control and diabetic, wild-type and Esm-1 knockout mice. Open circles, control mice; closed circles, diabetic (DM) mice. Black, wild-type (WT) littermate controls; gray, Esm-1 knockout (KO) mice. In all panels except (D), results are presented per mouse and include mean±SEM. In panel (D), results are presented as mean±SEM. $n=$ 6–11 mice per group. *$P<0.05$ compared across groups as indicated, #$P<0.05$ versus control mice by two-way ANOVA.

matrix proteins at the time of euthanasia, as compared with diabetes alone (Supplemental Figure 10, Supplemental Appendix 1). Taken together, overexpression of Esm-1 preserves podocyte health.

Esm-1 Attenuates IFN Signaling in DKD

To understand the mechanism of how Esm-1 significantly prevents diabetes-induced kidney injury, we explored transcriptomic responses in glomeruli (Supplemental Figure 11). Using bulk RNAseq, diabetic mice

demonstrate several pathways that are up- and downregulated (Figure 6A). Strikingly, of the top 11 highly enriched and significantly upregulated pathways, seven of these relate to IFN signaling. When we compare control versus diabetic mice with overexpression of mouse Esm-1, the majority of these pathways, except IFN-β, are not enriched. No pathways were significantly enriched in the direct comparison of diabetic mice with overexpression of Esm-1 versus diabetes alone. However, when we analyze by individual IFN-related genes from these significant pathways, of the 106 genes that are differentially expressed, 105 are upregulated in
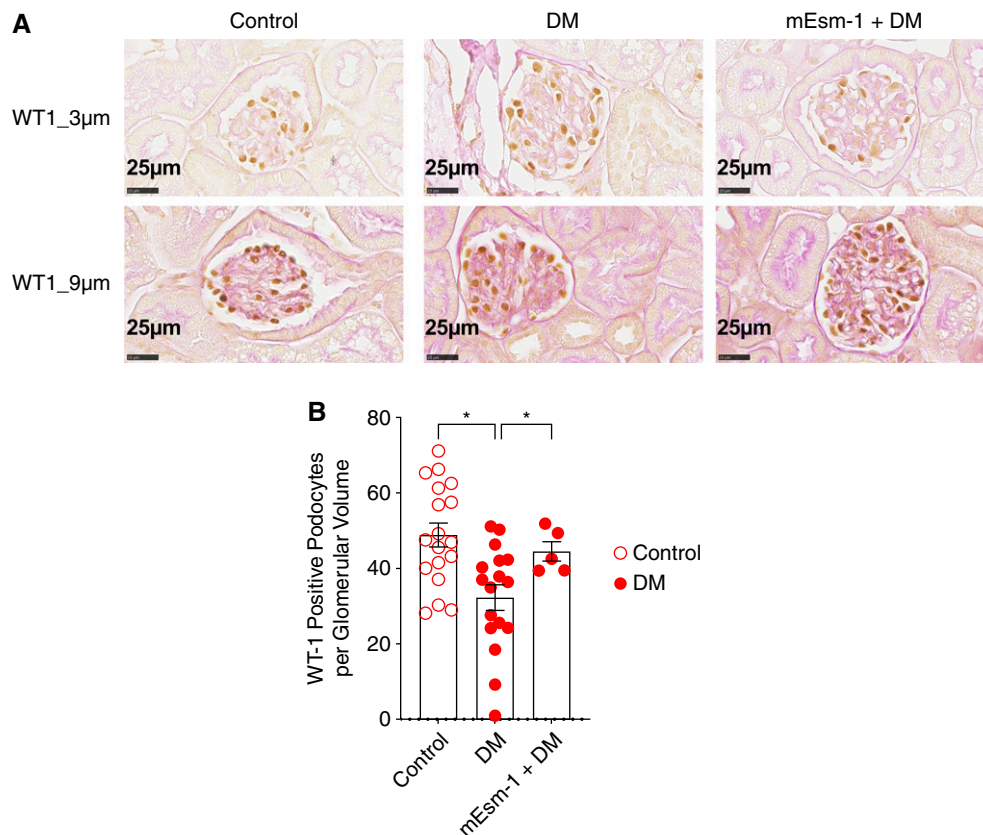
Figure 5. | **Systemic overexpression of mouse Esm-1 restores podocyte loss induced by diabetes.** (A) Representative images of mouse kidney sections stained for WT-1 expression. Scale bars (black) as indicated. (B) WT-1(+) podocytes per glomerulus on larger cohort mice. Open circles, control mice; closed circles, diabetic (DM) mice. $n=5–18$ mice per group. *$P<0.05$ compared across groups, as indicated by one-way ANOVA. m, mouse.

diabetes versus control mice. Of these upregulated IFN-related genes, 87 are modestly downregulated in samples from diabetic mice with overexpression of Esm-1 versus diabetes alone. Nineteen of these downregulated genes have q-values <0.05 and, by fold change, the most significantly downregulated gene with Esm-1 treatment is *Cxcl11* (33,34) (Supplemental Figure 12). In an orthogonal analysis of the most up- or downregulated genes between diabetes with overexpression of Esm-1 versus diabetes alone, we detect 41 significantly and differentially expressed genes (Figure 6B). From this list, we note several solute carriers, but also honed in on genes with known association with kidney disease and IFN signaling: *Ackr2* (35) and *Cxcl11* (33, 34). *Ackr2* and *Cxcl11* are significantly downregulated with overexpression of Esm-1 (Figure 6, C and D), and we validate these findings by quantitative PCR in a larger cohort of mice (2.17 ± 0.36 versus 0.42 ± 0.064, $P<0.001$ for *Acrk2* and 9.2 ± 1.3 versus 2.4 ± 0.32, $P<0.001$ for *Cxcl11*; Figure 6, E and F).

### Esm-1 Deficiency Predicts Progressive Stages of Albuminuria in Patients with Diabetes

To determine whether our observations in mice extend to humans, we measured circulating Esm-1 in patients with and without DKD. Among patients with diabetes, those with micro- or macroalbuminuria demonstrate significantly

lower eGFR than those with normoalbuminuria (Table 1, Supplemental Figure 13). In a cross-sectional analysis, circulating Esm-1 does not inversely correlate with kidney injury, although the level of Esm-1 may be confounded by stage of CKD (Figure 7). However, in a prospective study, patients with normo- or microalbuminuria that progressed to micro- or macroalbuminuria have significantly lower baseline Esm-1 (median [interquartile range], 5.1 [1.3] versus 6.8 [3.7] ng/ml; $P=0.007$; Figure 7, Table 2).

Discussion

In DKD-susceptible mice, we found a wide range for measures of kidney injury and that plasma Esm-1 modulates this association. Plasma Esm-1 >3 ng/ml correlates with protection from albuminuria and glomerular leukocyte infiltration (Figures 1 and 2). These data suggest at least two potential interpretations: (1) Esm-1 protects from worsening DKD, or (2) Esm-1 is a marker but not a mediator of DKD. To distinguish between these possibilities and to determine causality *in vivo*, we used overexpression and knockout approaches. We demonstrate that circulating Esm-1 is sufficient for renoprotection in DKD-susceptible mice (Figures 3 and 8). Complementary knockout experiments on a DKD-resistant background are congruent with results from overexpression experiments; however, the
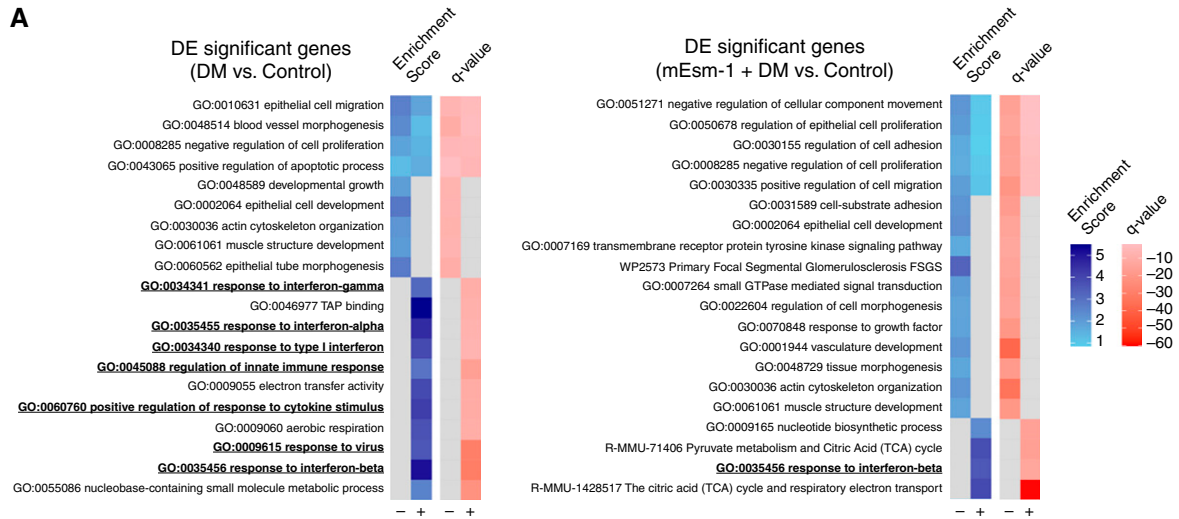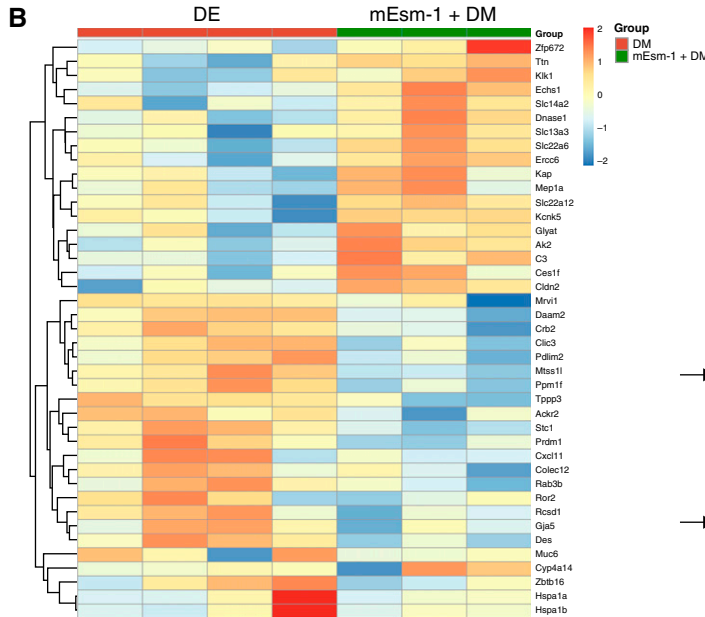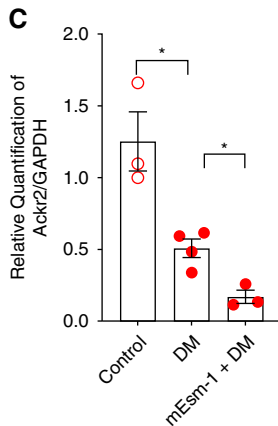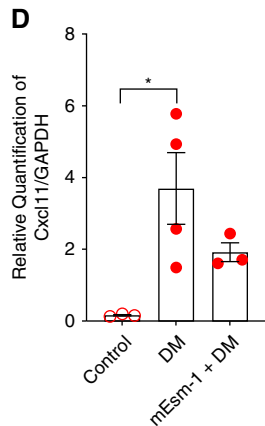
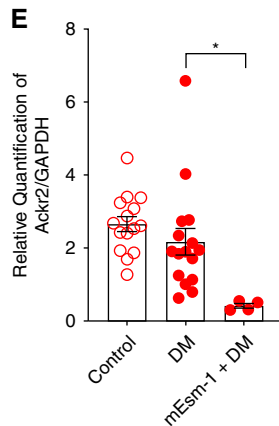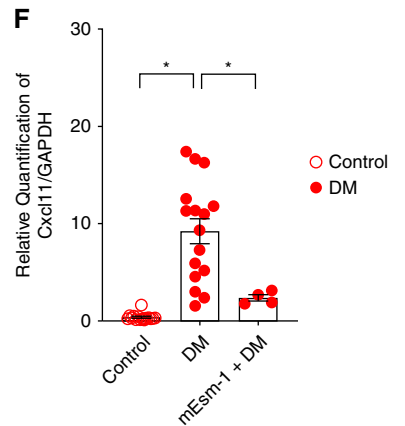**Figure 6. | Esm-1 attenuates chemokine/chemokine receptor expression in glomeruli.** (A) Heat maps of enrichment of ontology clusters, showing the hypergeometric q-values of Gene Ontology (GO) terms falling into each term for the top 20 most significantly enriched ontology clusters in each gene list. We performed a hierarchic clustering of significant ontology terms into a tree based on κ-statistical similarities among their gene memberships. We selected the term with the best q-value within each differentially expressed (DE) cluster as its

effect of Esm-1 deletion is modest (Figures 4 and 8). Although one may anticipate that Esm-1 deletion would not reduce glomerular leukocyte infiltration, in constitutive knockout mice, we must account for the role of Esm-1 in vascular development (18). Indeed, Rocha *et al.* (18) showed that constitutive Esm-1 knockout mice had a higher trans-cellular resistance and, in an acute model of leukocyte infil-tration, were also protected from inflammation.

As evidenced by *in vitro* and *in vivo* studies, the anti-inflammatory mechanisms of Esm-1 are noted in other sys-tems but have not been shown in glomeruli or in chronic conditions, such as diabetes. Esm-1 treatment both *in vitro* and *in vivo* reduces leukocyte infiltration acutely. Esm-1 binds to LFA-1 on Jurkat T cells, and blocks the LFA-1 and intercellular adhesion molecule-1 interaction (17). We have previously shown that Esm-1 inhibits human leukocyte transmigration, but not adhesion, in a microfluidic flow chamber assay *ex vivo* (11). Intraperitoneal injection of human Esm-1 in Balb/c mice 1 hour after LPS administra-tion mildly, but significantly, decreased lung neutrophil infiltration *in vivo* (15). However, our results show that, in mice, Esm-1 inversely correlates with, but does not consis-tently inhibit, leukocyte infiltration in kidney tissue several weeks after the onset of diabetes. Possible explanations for this observation include: (1) Esm-1 has some differential functions across species (*e.g.,* due to differential rates of gly-cosylation) (36); (2) constitutive Esm-1 may determine leuko-cyte infiltration, and we overexpressed Esm-1 in adulthood; (3) Esm-1 may reduce distinct subtypes of macrophages (37) and further leukocyte phenotyping is needed; (4) Esm-1 only alters the amount of resident leukocytes (*e.g.,* macrophages); and/or (5) compensatory mechanisms overcome acute effects of Esm-1, and chronic effects of Esm-1 are on structural features of DKD downstream of infiltrating leukocytes.

Endogenous Esm-1 is primarily localized to glomeruli, and DKD-susceptible mice have a baseline deficiency of Esm-1, specifically in glomeruli. Moreover, although hyper-glycemia increases glomerular Esm-1 production, this increase is markedly attenuated in DKD-susceptible mice (11). Thus, our data on circulating Esm-1 are consistent with previously published data on glomerular Esm-1. Although specific overexpression from glomerular endo-thelial cells was not technically feasible, in this study, we used hydrodynamic injection to overexpress Esm-1 and increase circulating Esm-1. Esm-1 is a locally derived inhibitor of inflammation and manipulating the level of this inhibitor is an attractive candidate approach to attenuate DKD, without the disadvantages of systemic immunosuppression. Our observation of different kidney phenotypes and transcriptomic changes in glomeruli implies direct effects of circulating Esm-1 on kidney, and motivates future studies to overexpress Esm-1 specifically in glomerular endothelial cells and across multiple mouse models of DKD and possibly other podocytopathies.

A glomerular signature of IFN-inducible genes that we observe in diabetic versus control mice is pathophysiologi-cally relevant for DKD. Several cytokine cascades in the pathogenesis of diabetic nephropathy (DN), including TNF-α, IL-6, and IL-18 (38–40), implicate IFN signaling. IL-18 is a predictor of albuminuria in type 2 diabetes melli-tus and DN (41, 42), and higher IL-18 levels are associated with more severe DN (43–45). The Nrlp3 inflammasome, which increases mature IL-18, aggravates DN (46). IL-18 is a prominent inducer of IFN-γ *via* NF-κB (47, 48), and NF-κB inhibition attenuates diabetic kidney injury (49). IFN-γ is upregulated in patients with diabetes and kidney disease compared with diabetes alone (50), and IFN-γ also upregu-lates the inflammasome (51). Toll-like receptors are acti-vated in human kidney and mediate the pathogenesis in rodent models of DN (52–54). When stimulated, these toll-like receptors stimulate gene transcription *via* NF-κB, such as the NF-κB target gene, type 1 IFN-β (55). Transcription of IFN-inducible genes are then synergistically stimulated by NF-κB and IFN signaling. Notably, genes upregulated in progressive human DKD share a well-recognized NF-κB– and IFN-response element (NFKB_IRFF_01) (56, 57). Therefore, one role for Esm-1 to mitigate DKD may be through its ability to attenuate the transcription of IFN-inducible genes. Interestingly, Esm-1 transcription is stimu-lated by several cytokines, but is inhibited by IFN-γ (16). On the basis of our data, one consequence of IFN-γ–mediated reduction of Esm-1 transcription may be more effective propagation of IFN signaling.

Another aspect of inflammation in DKD is upregulation of chemokines and adhesion molecules leading to leuko-cyte recruitment (38, 54). However, direct effects on glo-merular cell types (*e.g.,* podocyte apoptosis, mesangial matrix accumulation, and endothelial cell permeability) are also well-known characteristics of an inflammatory pheno-type (58, 59). For example, toll-like receptors and IFNs can mediate podocyte apoptosis (60–62). Moreover, the chemo-kine receptor CCR2, on macrophages, mediates leukocyte infiltration, but the same gene activated specifically on podocytes mediates podocytes apoptosis, independent of macrophage infiltration (59). Chronic overexpression of systemic Esm-1 inhibits albuminuria and structural features of DKD, but not inflammatory cell infiltration. Thus, the

---

Figure 6. | *Continued.* representative term and display it in the heat maps with enrichment score and q-value. Gray heat map cells repre-sent the nonsignificantly enriched ontology clusters in a given gene list. Light blue is lowest enrichment, dark blue is highest enrichment. Light red is lowest q-value, dark red is highest q-value. Pathways upregulated with diabetes or diabetes plus mouse Esm-1, relative to con-trol, are indicated by +; pathways downregulated with diabetes or diabetes plus mouse Esm-1, relative to control, are indicated by −. (B) Left panel shows heat map with hierarchic clustering of glomerular genes significantly differentially regulated in diabetic (DM) mice versus diabetic mice with overexpression of mouse Esm-1 (mEsm-1+DM). Colors in cells from individual mice represent z-scores relative to mean of DM group, scale on right. Right panel shows genes up- (green) or downregulated (red) in glomeruli from diabetes versus mEsm-1+DM with $\log_2$ fold change (FC), *P* values, and q-values. Arrows highlight chemokine/chemokine receptor genes, *Ackr2* and *Cxcl11*. (C–D) Validation by quantitative PCR of (C) *Ackr2* and (D) *Cxcl11* expression relative to glyceraldehyde-3-phosphate dehydroge-nase (GAPDH) in samples used for glomerular RNA sequencing. Open circles, control mice; closed circles, diabetic mice. *n*=3–4 mice per group. (E–F) Validation by quantitative PCR of (E) *Ackr2* and (F) *Cxcl11* expression relative to GAPDH in all samples from mouse over-expression experiments, phenotyped for clinical and histologic characteristics. *n*=9–15 mice per group. *$P<0.05$ as indicated.

Table 1.   Baseline characteristics of patients with diabetes mellitus by albuminuria

Characteristic	Normoalbuminuria	Microalbuminuria	Macroalbuminuria	P Value
N	54	23	22	
Men, n (%)	34 (63)	15 (65)	12 (55)	0.73
Age, yr	64 (14.8)	70 (16.7)	68 (20.2)	0.21
Hemoglobin A1c, %	6.5 (1.4)	6.7 (2.1)	6.9 (1.1)	0.38
eGFR, ml/min per 1.73 m^2	78.6 (33.6)	52.8 (22.6)[a]	49.7 (30.7)[a]	<0.001
Urine ACR, mg/g	21 (20.7)	89 (102.5)[a]	1256.5 (1863.6)[a,b]	<0.001
Total Esm-1, ng/ml	6.2 (4.0)	6.3 (3.7)	5 (5.1)	0.39

Data reported as median (interquartile range). ACR, albumin-creatinine ratio; Esm-1, endothelial cell-specific molecule-1.
[a]P<0.05 versus normoalbuminuria, Kruskal–Wallis test.
[b]P<0.05 versus microalbuminuria, Kruskal–Wallis test.
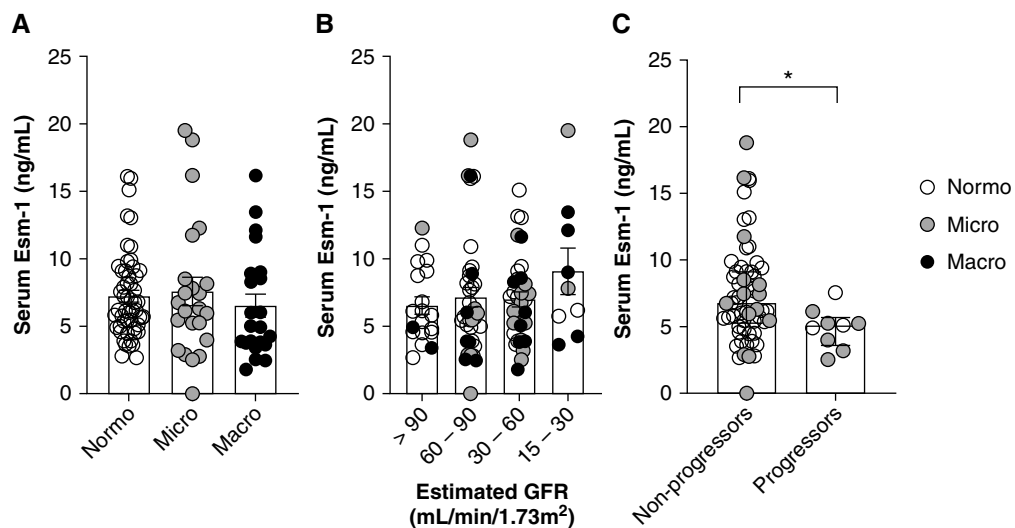
Figure 7. | Serum Esm-1 deficiency predicts progressive stages of albuminuria in patients with diabetes. (A) Level of circulating Esm-1 by classification of albuminuria. (B) Correlation of circulating Esm-1 with stages of CKD. (C) Level of circulating Esm-1 in nonprogressors and progressors. White circles, patients with diabetes with normoalbuminuria; gray circles, patients with microalbuminuria; black circles, patients with macroalbuminuria. Results are presented per patient and include mean±SEM. n=22–54 patients per classification of albuminuria. *P<0.05 versus nonprogressors by unpaired t test.

Table 2.   Baseline characteristics of patients with diabetes mellitus by progression status

Characteristic	Nonprogressors	Progressors	P Value
N	62	9	
Men, n (%)	41 (66)	4 (44)	0.30
Age, yr	64 (19.1)	66.0 (15.9)	0.28
Hemoglobin A1c, %	6.7 (1.7)	7.8 (1.9)	0.25
eGFR, ml/min per 1.73 m^2	77.1 (31.8)	54.2 (15.8)[a]	0.007
Urine ACR, mg/g	29.9 (19.8)	45 (70.7)[a]	0.01
Total Esm-1, ng/ml	6.8 (3.8)	5.1 (1.3)[a]	0.01

Data for age, hemoglobin A1c, eGFR, urine ACR, and total Esm-1 are reported as median (interquartile range). ACR, albumin-creatinine ratio; Esm-1, endothelial cell-specific molecule-1.
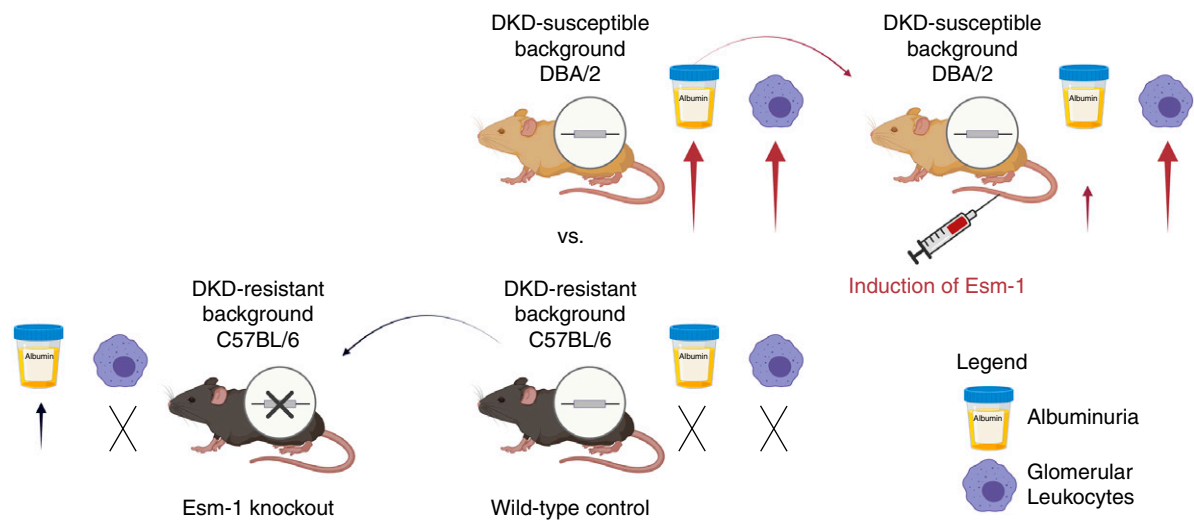[a]P<0.05 versus nonprogressors, Mann–Whitney test.

Figure 8. | **Overview of results with overexpression and deletion of Esm-1 in diabetic mice.** In DKD-susceptible mice (DBA/2), diabetes induces albuminuria and glomerular leukocyte infiltration in contrast to DKD-resistant mice (C57BL/6), with minimal albuminuria or infiltration. Induction of mouse or human Esm-1 in DKD-susceptible mice reduces albuminuria, independent of leukocyte infiltration. In contrast, Esm-1 deletion from DKD-resistant mice modestly increases albuminuria but not leukocyte infiltration. Arrows or "X" symbols indicate degree or absence of kidney injury, respectively, in diabetic mice relative to controls.

mechanisms of Esm-1 provide an example of separate but related pathways in DKD. Albuminuria and glomerular leukocyte infiltration do not correlate in our mouse model (Supplemental Figure 5). In prior human studies, leukocyte infiltration and albuminuria each correlate directly with tubulointerstitial fibrosis, but do not correlate directly with each other (63, 64), supporting the possibility that these important sequelae of kidney injury, at least in early DKD, may be, in part, due to separate mechanisms.

We validated selected target genes as potential mediators of the effects of Esm-1 on glomeruli. Two genes, *Ackr2* and *Cxcl11*, belong to a family of chemokines and chemokine receptors implicated in kidney disease and IFN signaling (34, 65–68). *Ackr2* can internalize chemokines for degradation, which reduces chemokine availability, inhibits leukocyte infiltration, and promotes immune resolution and adaptive immunity. However, the functions of *Ackr2* may be context dependent, and may be pathologic (35, 69, 70) or protective (35) in different disease models (71). Genetic deletion of *Ackr2* attenuates albuminuria, leukocyte infiltration, and IFN-related pathways (*e.g.*, NF-κB and pattern recognition receptors) in diabetic mice (35), suggesting loss of function of *Ackr2* is renoprotective in susceptible mice models of DKD (35). We similarly show that overexpression of Esm-1 downregulates glomerular *Ackr2* in diabetic DKD-susceptible mice, with attenuated albuminuria and attenuated IFN signaling. Cxcl11 and its receptor, Cxcr3, mediate chemotaxis and proliferation of immune cells in IFN-induced inflammation (34, 68, 72). In patients with CKD, urine Cxcl11 is higher in later stages of DKD and correlates with progression of disease (33). Additional ligands for Cxcr3 are upregulated in sera from patients with DKD versus those with diabetes alone (44). In patients with high- versus low-risk variants of IFN-induced APOL1, transcriptomic data show upregulation of glomerular *Cxcl11* (73, 74). In a mouse model of acute glomerular inflammation, systemic genetic deletion of Cxcr3 attenuates

glomerulosclerosis and albuminuria (75). Notably, Cxcl11 is not functional in DKD-resistant mice (C57BL/6) (76) due to insertion of two nucleotides and a resultant premature stop codon and nonsense-mediated decay. Different mouse strains susceptible to DKD, including DBA/2 and BALB/c (8, 9), produce a functional copy of *Cxcl11*. A nonfunctional allele of *Cxcl11* in C57BL/6 mice may be an explanation for why Esm-1 deletion may only have a modest permissive effect on albuminuria on this background strain because deletion could not reciprocally increase *Cxcl11*. In future studies to assess the protective role of Esm-1, we will characterize the contribution of these chemokine-related genes and other differentially regulated genes in IFN-dependent and IFN-independent pathways.

Integration of our histologic and transcriptomic data suggests Esm-1 may more potently attenuate the parietal versus visceral podocyte apoptosis of diabetes (77, 78). We show that Esm-1 attenuates multiple IFN-stimulated glomerular genes, including *Cxcl11*, but fewer genes from the IFN-β pathway (Figure 6, Supplemental Figure 12). IFN-α, compared to IFN-β, markedly stimulates kidney *Cxcl11* (62). IFN-α, in contrast to IFN-β, also induces apoptosis in parietal versus visceral podocytes *in vitro* and *in vivo* (62). In histologic studies, differences in the protective effect of Esm-1 on WT-1(+) versus p57(+) podocytes may be driven by effects on parietal podocytes, because WT-1 expression is more pronounced in these cells compared with p57 (Figure 5, Supplemental Figures 8 and 9). Thus, Esm-1–mediated attenuation of IFN-α and *Cxcl11* may be one mechanism to preserve parietal podocyte integrity and to reduce albuminuria.

Although others have reported correlations of Esm-1 with kidney diseases (79–82), cardiovascular diseases (79, 83–86), and cancer (87–91), data linking Esm-1 to DKD have been mixed. For example, Ekiz-Bilir *et al.* (92) showed a direct correlation between serum Esm-1 and the degree of albuminuria in patients with type 2 diabetes mellitus,

whereas Cikrikcioglu *et al.* (93) reported the opposite. Using cross-sectional data, we do not observe a lower circulating level of Esm-1 in patients with diabetes and albuminuria. However, in longitudinal outcomes in patients with minimal initial kidney injury, circulating Esm-1 was lower in those patients that developed progressive stages of albuminuria (Figure 7). On the basis of potential confounding, and short duration of follow-up, these data require confirmation in a larger cohort with longer follow-up.

In summary, Esm-1 inversely correlates with DKD in mice and predicts protection from DKD in humans. We determine that Esm-1 rescues DKD-susceptible mice from podocyte injury and albuminuria, and Esm-1 deletion partially reverses the protective background of DKD-resistant mice. Esm-1 attenuates IFN-stimulated pathways and downregulates chemokine signaling, *e.g.*, glomerular *Acrk2* and *Cxcl11*, that are part of a potential mechanism to attenuate DKD. Taken together, upregulation of Esm-1 should be explored as a possible therapeutic strategy in DKD.

Disclosures

Funding

Acknowledgments

Author Contributions

A. Balistrieri, V. Bhalla, N. de Freitas Caires, A. Gaudet, L. Higdon, J.S. Maltzman, P. Nallagatla, A. Rosenberg, B. Santo, M. Shah, and X. Zheng were responsible for methodology; A. Balistrieri, V. Bhalla, N. de Freitas Caires, A. Gaudet, B. Ginley, C. Li, K. Myakala, P. Nadai, B. Santo, M. Shah, X.X. Wang, X. Yang, and X. Zheng were responsible for investigation; V. Bhalla, N. de Freitas Caires, A. Gaudet, L. Higdon, J.S. Maltzman, P. Nallagatla, L. Palaniappan, A. Rosenberg, B. Santo, M. Shah, X.X. Wang, and X. Zheng were responsible for formal analysis; V. Bhalla was responsible for project administration; V. Bhalla, N. de Freitas Caires, A. Gaudet, L. Higdon, M. Levi, J.S. Maltzman, L. Palaniappan, A. Rosenberg, and X. Zheng reviewed and edited the manuscript; V. Bhalla, N. de Freitas Caires, A. Gaudet, L. Higdon, and X. Zheng were responsible for validation; V. Bhalla, A. Gaudet, L. Higdon, P. Nallagatla, L. Palaniappan, M. Shah, and X. Zheng were responsible for data curation; V. Bhalla, N. de Freitas Caires, L. Higdon, M. Levi, J.S. Maltzman, A. Rosenberg, P. Sarder, and X. Zheng conceptualized the study; V. Bhalla, N. de Freitas Caires, M. Levi, J.S. Maltzman, A. Rosenberg, and P. Sarder provided supervision; V. Bhalla and X. Zheng wrote the original draft and were responsible for funding acquisition; N. de Freitas Caires, L. Higdon, P. Nadai, P. Nallagatla, and L. Palaniappan were responsible for resources;

A. Gaudet, P. Nallagatla, and B. Santo were responsible for software; and A. Gaudet, B. Santo, and X. Zheng were responsible for visualization.

Data Sharing Statement

We submitted the data from our RNAseq experiments to Geobank (accession number GSE175449).

Supplemental Material

This article contains the following supplemental material online at http://kidney360.asnjournals.org/lookup/suppl/doi:10.34067/KID.0001712022/-/DCSupplemental.

Supplemental Appendix 1. Supplemental methods.

Supplemental Appendix 2. Supplemental references.

Supplemental Table 1. Antibodies for flow cytometry experiments.

Supplemental Table 2. Genotyping primer sequences for Esm-1 knockout mice.

Supplemental Table 3. RT-qPCR primer sequences for validation of bulk RNAseq.

Supplemental Table 4. Podometric data.

Supplemental Figure 1. Quantification of glomerular leukocytes and leukocyte subsets.

Supplemental Figure 2. Intraperitoneal injection of recombinant protein only transiently increases circulating mouse Esm-1.

Supplemental Figure 3. Hydrodynamic injection induces over-expression in hepatocytes and a stable increase in circulating Esm-1.

Supplemental Figure 4. Over-expression of Esm-1 and leukocyte subsets in glomerular and tubulointerstitial compartments in diabetic DKD-susceptible mice.

Supplemental Figure 5. Correlation of glomerular leukocyte infiltration and albuminuria in DKD-susceptible mice.

Supplemental Figure 6. Schematic design of Esm-1 knockout mice.

Supplemental Figure 7. Constitutive deletion of Esm-1 and leukocyte subsets in glomerular and tubulointerstitial compartments in diabetic DKD-resistant mice.

Supplemental Figure 8. Parietal and visceral podocyte markers in mouse kidney.

Supplemental Figure 9. Systemic over-expression of mouse Esm-1 attenuates podocyte injury induced by diabetes.

Supplemental Figure 10. Systemic over-expression of mouse Esm-1 does not influence glomerular extracellular matrix deposition induced by diabetes.

Supplemental Figure 11. Clinical and histologic characteristics of mice utilized for glomerular RNAseq.

Supplemental Figure 12. Esm-1 attenuates diabetes-induced interferon signaling in glomeruli.

Supplemental Figure 13. Characteristics of patients with diabetes.

References

1. Parving HH, Hommel E, Mathiesen E, Skøtt P, Edsberg B, Bahnsen M, Lauritzen M, Hougaard P, Lauritzen E: Prevalence of microalbuminuria, arterial hypertension, retinopathy and neuropathy in patients with insulin dependent diabetes. *Br Med J (Clin Res Ed)* 296: 156–160, 1988 https://doi.org/10.1136/bmj.296.6616.156

2. Borch-Johnsen K, Andersen PK, Deckert T: The effect of proteinuria on relative mortality in type 1 (insulin-dependent) diabetes mellitus. *Diabetologia* 28: 590–596, 1985 https://doi.org/10.1007/BF00281993

3. Rossing P, Hougaard P, Borch-Johnsen K, Parving HH: Predictors of mortality in insulin dependent diabetes: 10 year observational follow up study. *BMJ* 313: 779–784, 1996 https://doi.org/10.1136/bmj.313.7060.779

4. Kramer HJ, Nguyen QD, Curhan G, Hsu CY: Renal insufficiency in the absence of albuminuria and retinopathy among adults with type 2 diabetes mellitus. *JAMA* 289: 3273–3277, 2003 https://doi.org/10.1001/jama.289.24.3273

5. Lachin JM, Genuth S, Cleary P, Davis MD, Nathan DM; Diabetes Control and Complications Trial/Epidemiology of Diabetes Interventions and Complications Research Group: Retinopathy and nephropathy in patients with type 1 diabetes four years after a trial of intensive therapy. *N Engl J Med* 342: 381–389, 2000 https://doi.org/10.1056/NEJM200002103420603

6. de Boer IH, Sun W, Cleary PA, Lachin JM, Molitch ME, Steffes MW, Zinman B; DCCT/EDIC Research Group: Intensive diabetes therapy and glomerular filtration rate in type 1 diabetes. *N Engl J Med* 365: 2366–2376, 2011 https://doi.org/10.1056/NEJMoa1111732

7. Adler AI, Stevens RJ, Manley SE, Bilous RW, Cull CA, Holman RR; UKPDS GROUP: Development and progression of nephropathy in type 2 diabetes: The United Kingdom Prospective Diabetes Study (UKPDS 64). *Kidney Int* 63: 225–232, 2003 https://doi.org/10.1046/j.1523-1755.2003.00712.x

8. Gurley SB, Clare SE, Snow KP, Hu A, Meyer TW, Coffman TM: Impact of genetic background on nephropathy in diabetic mice. *Am J Physiol Renal Physiol* 290: F214–F222, 2006 https://doi.org/10.1152/ajprenal.00204.2005

9. Qi Z, Fujita H, Jin J, Davis LS, Wang Y, Fogo AB, Breyer MD: Characterization of susceptibility of inbred mouse strains to diabetic nephropathy. *Diabetes* 54: 2628–2637, 2005 https://doi.org/10.2337/diabetes.54.9.2628

10. Bhalla V, Velez MG, Chertow GM: A transcriptional blueprint for human and murine diabetic kidney disease. *Diabetes* 62: 31–33, 2013 https://doi.org/10.2337/db12-1121

11. Zheng X, Soroush F, Long J, Hall ET, Adishesha PK, Bhattacharya S, Kiani MF, Bhalla V: Murine glomerular transcriptome links endothelial cell-specific molecule-1 deficiency with susceptibility to diabetic nephropathy. *PLoS One* 12: e0185250, 2017 https://doi.org/10.1371/journal.pone.0185250

12. Qi H, Casalena G, Shi S, Yu L, Ebefors K, Sun Y, Zhang W, D'Agati V, Schlondorff D, Haraldsson B, Böttinger E, Daehn I: Glomerular endothelial mitochondrial dysfunction is essential and characteristic of diabetic kidney disease susceptibility. *Diabetes* 66: 763–778, 2017 https://doi.org/10.2337/db16-0695

13. Galkina E, Ley K: Leukocyte recruitment and vascular injury in diabetic nephropathy. *J Am Soc Nephrol* 17: 368–377, 2006 https://doi.org/10.1681/ASN.2005080859

14. Moore KJ, Tabas I: Macrophages in the pathogenesis of atherosclerosis. *Cell* 145: 341–355, 2011 https://doi.org/10.1016/j.cell.2011.04.005

15. Gaudet A, Portier L, Prin M, Copin MC, Tsicopoulos A, Mathieu D, Lassalle P, De Freitas Caires N: Endocan regulates acute lung inflammation through control of leukocyte diapedesis. *J Appl Physiol (1985)* 127: 668–678, 2019 https://doi.org/10.1152/japplphysiol.00337.2019

16. Lassalle P, Molet S, Janin A, Heyden JV, Tavernier J, Fiers W, Devos R, Tonnel AB: ESM-1 is a novel human endothelial cell-specific molecule expressed in lung and regulated by cytokines. *J Biol Chem* 271: 20458–20464, 1996 https://doi.org/10.1074/jbc.271.34.20458

17. Béchard D, Scherpereel A, Hammad H, Gentina T, Tsicopoulos A, Aumercier M, Pestel J, Dessaint JP, Tonnel AB, Lassalle P: Human endothelial-cell specific molecule-1 binds directly to the integrin CD11a/CD18 (LFA-1) and blocks binding to intercellular adhesion molecule-1. *J Immunol* 167: 3099–3106, 2001 https://doi.org/10.4049/jimmunol.167.6.3099

18. Rocha SF, Schiller M, Jing D, Li H, Butz S, Vestweber D, Biljes D, Drexler HC, Nieminen-Kelhä M, Vajkoczy P, Adams S, Benedito R, Adams RH: Esm1 modulates endothelial tip cell behavior and vascular permeability by enhancing VEGF bioavailability. *Circ Res* 115: 581–590, 2014 https://doi.org/10.1161/CIRCRESAHA.115.304718

19. Pan Y, Jiang S, Hou Q, Qiu D, Shi J, Wang L, Chen Z, Zhang M, Duan A, Qin W, Zen K, Liu Z: Dissection of glomerular

transcriptional profile in patients with diabetic nephropathy: SRGAP2a protects podocyte structure and function. *Diabetes* 67: 717–730, 2018 https://doi.org/10.2337/db17-0755

20. Wilson PC, Wu H, Kirita Y, Uchimura K, Ledru N, Rennke HG, Welling PA, Waikar SS, Humphreys BD: The single-cell transcriptomic landscape of early human diabetic nephropathy. *Proc Natl Acad Sci U S A* 116: 19619–19625, 2019 https://doi.org/10.1073/pnas.1908706116

21. Wang XX, Jiang T, Shen Y, Caldas Y, Miyazaki-Anzai S, Santamaria H, Urbanek C, Solis N, Scherzer P, Lewis L, Gonzalez FJ, Adorini L, Pruzanski M, Kopp JB, Verlander JW, Levi M: Diabetic nephropathy is accelerated by farnesoid X receptor deficiency and inhibited by farnesoid X receptor activation in a type 1 diabetes model. *Diabetes* 59: 2916–2927, 2010 https://doi.org/10.2337/db10-0019

22. Hazra S, Rasheed A, Bhatwadekar A, Wang X, Shaw LC, Patel M, Caballero S, Magomedova L, Solis N, Yan Y, Wang W, Thinschmidt JS, Verma A, Li Q, Levi M, Cummins CL, Grant MB: Liver X receptor modulates diabetic retinopathy outcome in a mouse model of streptozotocin-induced diabetes. *Diabetes* 61: 3270–3279, 2012 https://doi.org/10.2337/db11-1596

23. Mátés L, Chuah MK, Belay E, Jerchow B, Manoj N, Acosta-Sanchez A, Grzela DP, Schmitt A, Becker K, Matrai J, Ma L, Samara-Kuko E, Gysemans C, Pryputniewicz D, Miskey C, Fletcher B, VandenDriessche T, Ivics Z, Izsvák Z: Molecular evolution of a novel hyperactive Sleeping Beauty transposase enables robust stable gene transfer in vertebrates. *Nat Genet* 41: 753–761, 2009 https://doi.org/10.1038/ng.343

24. Hartleben B, Widmeier E, Wanner N, Schmidts M, Kim ST, Schneider L, Mayer B, Kerjaschki D, Miner JH, Walz G, Huber TB: Role of the polarity protein Scribble for podocyte differentiation and maintenance [published correction appears in *PLoS One* 9, 2014 10.1371/annotation/2c0c1c61-0627-4794-b6f2-01fc4db84dcb]. *PLoS One* 7: e36705, 2012 https://doi.org/10.1371/journal.pone.0036705

25. American Diabetes Association: Diagnosis and classification of diabetes mellitus. *Diabetes Care* 33: S62–S69, 2010 https://doi.org/10.2337/dc10-S062

26. Levey AS, Stevens LA, Schmid CH, Zhang YL, Castro AF 3rd, Feldman HI, Kusek JW, Eggers P, Van Lente F, Greene T, Coresh J; CKD-EPI (Chronic Kidney Disease Epidemiology Collaboration): A new equation to estimate glomerular filtration rate. *Ann Intern Med* 150: 604–612, 2009 https://doi.org/10.7326/0003-4819-150-9-200905050-00006

27. Zhou Y, Zhou B, Pache L, Chang M, Khodabakhshi AH, Tanaseichuk O, Benner C, Chanda SK: Metascape provides a biologist-oriented resource for the analysis of systems-level datasets. *Nat Commun* 10: 1523, 2019 https://doi.org/10.1038/s41467-019-09234-6

28. Chen CA, Carolan PJ, Annes JP: In vivo screening for secreted proteins that modulate glucose handling identifies interleukin-6 family members as potent hypoglycemic agents [published correction appears in PLoS One 7, 2012 10.1371/annotation/6e392eb7-55cb-4bc6-ab8e-bd8130ad6582]. *PLoS One* 7: e44600, 2012 https://doi.org/10.1371/journal.pone.0044600

29. Hiromura K, Haseley LA, Zhang P, Monkawa T, Durvasula R, Petermann AT, Alpers CE, Mundel P, Shankland SJ: Podocyte expression of the CDK-inhibitor p57 during development and disease. *Kidney Int* 60: 2235–2246, 2001 https://doi.org/10.1046/j.1523-1755.2001.00057.x

30. Nagata M, Shibata S, Shigeta M, Yu-Ming S, Watanabe T: Cyclin-dependent kinase inhibitors: p27kip1 and p57kip2 expression during human podocyte differentiation. *Nephrol Dial Transplant* 14: 48–51, 1999 https://doi.org/10.1093/ndt/14.suppl_1.48

31. Puelles VG, van der Wolde JW, Schulze KE, Short KM, Wong MN, Bensley JG, Cullen-McEwen LA, Caruana G, Hokke SN, Li J, Firth SD, Harper IS, Nikolic-Paterson DJ, Bertram JF: Validation of a three-dimensional method for counting and sizing podocytes in whole glomeruli. *J Am Soc Nephrol* 27: 3093–3104, 2016 https://doi.org/10.1681/ASN.2015121340

32. Wang Z, Jiang T, Li J, Proctor G, McManaman JL, Lucia S, Chua S, Levi M: Regulation of renal lipid metabolism, lipid accumulation, and glomerulosclerosis in FVBdb/db mice with type 2 diabetes. *Diabetes* 54: 2328–2335, 2005 https://doi.org/10.2337/diabetes.54.8.2328

33. Lebherz-Eichinger D, Klaus DA, Reiter T, Horl WH, Haas M, Ankersmit HJ, Krenn CG, Roth GA: Increased chemokine excretion in patients suffering from chronic kidney disease. *Transl Res* 164: 433–443.e1-2, 2014 https://doi.org/10.1016/j.trsl.2014.07.004

34. Metzemaekers M, Vanheule V, Janssens R, Struyf S, Proost P: Overview of the mechanisms that may contribute to the non-redundant activities of interferon-inducible CXC chemokine receptor 3 ligands. *Front Immunol* 8: 1970, 2018 https://doi.org/10.3389/fimmu.2017.01970

35. Zheng S, Coventry S, Cai L, Powell DW, Jala VR, Haribabu B, Epstein PN: Renal protection by genetic deletion of the atypical chemokine receptor ACKR2 in diabetic OVE mice. *J Diabetes Res* 2016: 5362506, 2016 https://doi.org/10.1155/2016/5362506

36. De Freitas Caires N, Lassalle P: Highlight on mouse endocan. *Circ Res* 116: e69–e70, 2015 https://doi.org/10.1161/CIRCRESAHA.115.306353

37. You H, Gao T, Cooper TK, Brian Reeves W, Awad AS: Macrophages directly mediate diabetic renal injury. *Am J Physiol Renal Physiol* 305: F1719–F1727, 2013 https://doi.org/10.1152/ajprenal.00141.2013

38. Navarro-González JF, Mora-Fernández C: The role of inflammatory cytokines in diabetic nephropathy. *J Am Soc Nephrol* 19: 433–442, 2008 https://doi.org/10.1681/ASN.2007091048

39. Yaribeygi H, Atkin SL, Sahebkar A: Interleukin-18 and diabetic nephropathy: A review. *J Cell Physiol* 234: 5674–5682, 2019 https://doi.org/10.1002/jcp.27427

40. Gurley SB, Ghosh S, Johnson SA, Azushima K, Sakban RB, George SE, Maeda M, Meyer TW, Coffman TM: Inflammation and immunity pathways regulate genetic susceptibility to diabetic nephropathy. *Diabetes* 67: 2096–2106, 2018 https://doi.org/10.2337/db17-1323

41. Nakamura A, Shikata K, Hiramatsu M, Nakatou T, Kitamura T, Wada J, Itoshima T, Makino H: Serum interleukin-18 levels are associated with nephropathy and atherosclerosis in Japanese patients with type 2 diabetes. *Diabetes Care* 28: 2890–2895, 2005 https://doi.org/10.2337/diacare.28.12.2890

42. Araki S, Haneda M, Koya D, Sugimoto T, Isshiki K, Chin-Kanasaki M, Uzu T, Kashiwagi A: Predictive impact of elevated serum level of IL-18 for early renal dysfunction in type 2 diabetes: An observational follow-up study. *Diabetologia* 50: 867–873, 2007 https://doi.org/10.1007/s00125-006-0586-8

43. Moriwaki Y, Yamamoto T, Shibutani Y, Aoki E, Tsutsumi Z, Takahashi S, Okamura H, Koga M, Fukuchi M, Hada T: Elevated levels of interleukin-18 and tumor necrosis factor-alpha in serum of patients with type 2 diabetes mellitus: Relationship with diabetic nephropathy. *Metabolism* 52: 605–608, 2003 https://doi.org/10.1053/meta.2003.50096

44. Wong CK, Ho AW, Tong PC, Yeung CY, Kong AP, Lun SW, Chan JC, Lam CW: Aberrant activation profile of cytokines and mitogen-activated protein kinases in type 2 diabetic patients with nephropathy. *Clin Exp Immunol* 149: 123–131, 2007 https://doi.org/10.1111/j.1365-2249.2007.03389.x

45. Fujita T, Ogihara N, Kamura Y, Satomura A, Fuke Y, Shimizu C, Wada Y, Matsumoto K: Interleukin-18 contributes more closely to the progression of diabetic nephropathy than other diabetic complications. *Acta Diabetol* 49: 111–117, 2012 https://doi.org/10.1007/s00592-010-0178-4

46. Shahzad K, Bock F, Dong W, Wang H, Kopf S, Kohli S, Al-Dabet MM, Ranjan S, Wolter J, Wacker C, Biemann R, Stoyanov S, Reymann K, Söderkvist P, Groß O, Schwenger V, Pahernik S, Nawroth PP, Gröne HJ, Madhusudhan T, Isermann B: Nlrp3-inflammasome activation in non-myeloid-derived cells aggravates diabetic nephropathy. *Kidney Int* 87: 74–84, 2015 https://doi.org/10.1038/ki.2014.271

47. Okamura H, Tsutsi H, Komatsu T, Yutsudo M, Hakura A, Tanimoto T, Torigoe K, Okura T, Nukada Y, Hattori K, Akita K, Namba M, Tanabe F, Konishi K, Fukuda S, Kurimoto M: Cloning of a new cytokine that induces IFN-gamma production by T cells. *Nature* 378: 88–91, 1995 https://doi.org/10.1038/378088a0

48. Kojima H, Aizawa Y, Yanai Y, Nagaoka K, Takeuchi M, Ohta T, Ikegami H, Ikeda M, Kurimoto M: An essential role for

NF-kappa B in IL-18-induced IFN-gamma expression in KG-1 cells. *J Immunol* 162: 5063–5069, 1999

49. Kim JE, Lee MH, Nam DH, Song HK, Kang YS, Lee JE, Kim HW, Cha JJ, Hyun YY, Han SY, Han KH, Han JY, Cha DR: Celastrol, an NF-κB inhibitor, improves insulin resistance and attenuates renal injury in db/db mice. *PLoS One* 8: e62068, 2013 https://doi.org/10.1371/journal.pone.0062068

50. Aly RH, Ahmed AE, Hozayen WG, Rabea AM, Ali TM, El Askary A, Ahmed OM: Patterns of Toll-like receptor expressions and inflammatory cytokine levels and their implications in the progress of insulin resistance and diabetic nephropathy in type 2 diabetic patients. *Front Physiol* 11: 609223, 2020 https://doi.org/10.3389/fphys.2020.609223

51. Kopitar-Jerala N: The role of interferons in inflammation and inflammasome activation. *Front Immunol* 8: 873, 2017 https://doi.org/10.3389/fimmu.2017.00873

52. Kuwabara T, Mori K, Mukoyama M, Kasahara M, Yokoi H, Nakao K: Macrophage-mediated glucolipotoxicity via myeloid-related protein 8/toll-like receptor 4 signaling in diabetic nephropathy. *Clin Exp Nephrol* 18: 584–592, 2014 https://doi.org/10.1007/s10157-013-0922-5

53. Mudaliar H, Pollock C, Panchapakesan U: Role of Toll-like receptors in diabetic nephropathy. *Clin Sci (Lond)* 126: 685–694, 2014 https://doi.org/10.1042/CS20130267

54. Pichler R, Afkarian M, Dieter BP, Tuttle KR: Immunity and inflammation in diabetic kidney disease: Translating mechanisms to biomarkers and treatment targets. *Am J Physiol Renal Physiol* 312: F716–F731, 2017 https://doi.org/10.1152/ajprenal.00314.2016

55. Uematsu S, Akira S: Toll-like receptors and type I interferons. *J Biol Chem* 282: 15319–15323, 2007 https://doi.org/10.1074/jbc.R700009200

56. Schmid H, Boucherot A, Yasuda Y, Henger A, Brunner B, Eichinger F, Nitsche A, Kiss E, Bleich M, Gröne HJ, Nelson PJ, Schlöndorff D, Cohen CD, Kretzler M; European Renal cDNA Bank (ERCB) Consortium: Modular activation of nuclear factor-kappaB transcriptional programs in human diabetic nephropathy. *Diabetes* 55: 2993–3003, 2006 https://doi.org/10.2337/db06-0477

57. Johnson DR, Pober JS: HLA class I heavy-chain gene promoter elements mediating synergy between tumor necrosis factor and interferons. *Mol Cell Biol* 14: 1322–1332, 1994 https://doi.org/10.1128/mcb.14.2.1322-1332.1994

58. Navarro-González JF, Mora-Fernández C, Muros de Fuentes M, García-Pérez J: Inflammatory molecules and pathways in the pathogenesis of diabetic nephropathy. *Nat Rev Nephrol* 7: 327–340, 2011 https://doi.org/10.1038/nrneph.2011.51

59. You H, Gao T, Raup-Konsavage WM, Cooper TK, Bronson SK, Reeves WB, Awad AS: Podocyte-specific chemokine (C-C motif) receptor 2 overexpression mediates diabetic renal injury in mice. *Kidney Int* 91: 671–682, 2017 https://doi.org/10.1016/j.kint.2016.09.042

60. Saurus P, Kuusela S, Lehtonen E, Hyvönen ME, Ristola M, Fogarty CL, Tienari J, Lassenius MI, Forsblom C, Lehto M, Saleem MA, Groop PH, Holthöfer H, Lehtonen S: Podocyte apoptosis is prevented by blocking the Toll-like receptor pathway. *Cell Death Dis* 6: e1752, 2015 https://doi.org/10.1038/cddis.2015.125

61. Xia H, Bao W, Shi S: Innate immune activity in glomerular podocytes. *Front Immunol* 8: 122, 2017 https://doi.org/10.3389/fimmu.2017.00122

62. Migliorini A, Angelotti ML, Mulay SR, Kulkarni OO, Demleitner J, Dietrich A, Sagrinati C, Ballerini L, Peired A, Shankland SJ, Liapis H, Romagnani P, Anders HJ: The antiviral cytokines IFN-α and IFN-β modulate parietal epithelial cells and promote podocyte loss: implications for IFN toxicity, viral glomerulonephritis, and glomerular regeneration. *Am J Pathol* 183: 431–440, 2013 https://doi.org/10.1016/j.ajpath.2013.04.017

63. Nguyen D, Ping F, Mu W, Hill P, Atkins RC, Chadban SJ: Macrophage accumulation in human progressive diabetic nephropathy. *Nephrology (Carlton)* 11: 226–231, 2006 https://doi.org/10.1111/j.1440-1797.2006.00576.x

64. Tesch GH: Macrophages and diabetic nephropathy. *Semin Nephrol* 30: 290–301, 2010 https://doi.org/10.1016/j.semnephrol.2010.03.007

65. Russo RC, Savino B, Mirolo M, Buracchi C, Germano G, Anselmo A, Zammataro L, Pasqualini F, Mantovani A, Locati M, Teixeira MM: The atypical chemokine receptor ACKR2 drives pulmonary fibrosis by tuning influx of CCR2$^+$ and CCR5$^+$ IFNγ-producing γδT cells in mice. *Am J Physiol Lung Cell Mol Physiol* 314: L1010–L1025, 2018 https://doi.org/10.1152/ajplung.00233.2017

66. Antonelli A, Ferrari SM, Mancusi C, Mazzi V, Pupilli C, Centanni M, Ferri C, Ferrannini E, Fallahi P: Interferon-α, -β and -γ induce CXCL11 secretion in human thyrocytes: modulation by peroxisome proliferator-activated receptor γ agonists. *Immunobiology* 218: 690–695, 2013 https://doi.org/10.1016/j.imbio.2012.08.267

67. Widney DP, Xia YR, Lusis AJ, Smith JB: The murine chemokine CXCL11 (IFN-inducible T cell alpha chemoattractant) is an IFN-gamma- and lipopolysaccharide-inducible glucocorticoid-attenuated response gene expressed in lung and other tissues during endotoxemia. *J Immunol* 164: 6322–6331, 2000 https://doi.org/10.4049/jimmunol.164.12.6322

68. Corbera-Bellalta M, Planas-Rigol E, Lozano E, Terrades-García N, Alba MA, Prieto-González S, García-Martínez A, Albero R, Enjuanes A, Espígol-Frigolé G, Hernández-Rodríguez J, Roux-Lombard P, Ferlin WG, Dayer JM, Kosco-Vilbois MH, Cid MC: Blocking interferon γ reduces expression of chemokines CXCL9, CXCL10 and CXCL11 and decreases macrophage infiltration in ex vivo cultured arteries from patients with giant cell arteritis. *Ann Rheum Dis* 75: 1177–1186, 2016 https://doi.org/10.1136/annrheumdis-2015-208371

69. Lux M, Blaut A, Eltrich N, Bideak A, Müller MB, Hoppe JM, Gröne HJ, Locati M, Vielhauer V: The atypical chemokine receptor 2 limits progressive fibrosis after acute ischemic kidney injury. *Am J Pathol* 189: 231–247, 2019 https://doi.org/10.1016/j.ajpath.2018.09.016

70. Bideak A, Blaut A, Hoppe JM, Müller MB, Federico G, Eltrich N, Gröne HJ, Locati M, Vielhauer V: The atypical chemokine receptor 2 limits renal inflammation and fibrosis in murine progressive immune complex glomerulonephritis. *Kidney Int* 93: 826–841, 2018 https://doi.org/10.1016/j.kint.2017.11.013

71. Bonavita O, Mollica Poeta V, Setten E, Massara M, Bonecchi R: ACKR2: An Atypical chemokine receptor regulating lymphatic biology. *Front Immunol* 7: 691, 2017 https://doi.org/10.3389/fimmu.2016.00691

72. Kuo PT, Zeng Z, Salim N, Mattarollo S, Wells JW, Leggatt GR: The role of CXCR3 and its chemokine ligands in skin disease and cancer. *Front Med (Lausanne)* 5: 271, 2018 https://doi.org/10.3389/fmed.2018.00271

73. Sampson MG, Robertson CC, Martini S, Mariani LH, Lemley KV, Gillies CE, Otto EA, Kopp JB, Randolph A, Vega-Warner V, Eichinger F, Nair V, Gipson DS, Cattran DC, Johnstone DB, O'Toole JF, Bagnasco SM, Song PX, Barisoni L, Troost JP, Kretzler M, Sedor JR; Nephrotic Syndrome Study Network: Integrative genomics identifies novel associations with APOL1 risk genotypes in Black NEPTUNE subjects. *J Am Soc Nephrol* 27: 814–823, 2016 https://doi.org/10.1681/ASN.2014111131

74. McNulty M, Fermin D, Eichinger F, Jang D, Kretzler M, Burtt N, Pollak MR, Flannick J, Weins A, Friedman DJ, Sampson MG; Nephrotic Syndrome Study Network (NEPTUNE): A glomerular transcriptomic landscape of APOL1 in Black patients with focal segmental glomerulosclerosis. *Kidney Int* 102: 136–148, 2022

75. Panzer U, Steinmetz OM, Paust HJ, Meyer-Schwesinger C, Peters A, Turner JE, Zahner G, Heymann F, Kurts C, Hopfer H, Helmchen U, Haag F, Schneider A, Stahl RA: Chemokine receptor CXCR3 mediates T cell recruitment and tissue injury in nephrotoxic nephritis in mice. *J Am Soc Nephrol* 18: 2071–2084, 2007 https://doi.org/10.1681/ASN.2006111237

76. Sierro F, Biben C, Martínez-Munoz L, Mellado M, Ransohoff RM, Li M, Woehl B, Leung H, Groom J, Batten M, Harvey RP, Martínez-A C, Mackay CR, Mackay F: Disrupted cardiac development but normal hematopoiesis in mice deficient in the second CXCL12/SDF-1 receptor, CXCR7. *Proc Natl Acad Sci U S A* 104: 14759–14764, 2007 https://doi.org/10.1073/pnas.0702229104

77. Kawaguchi T, Hasegawa K, Yasuda I, Muraoka H, Umino H, Tokuyama H, Hashiguchi A, Wakino S, Itoh H: Diabetic

condition induces hypertrophy and vacuolization in glomerular parietal epithelial cells. *Sci Rep* 11: 1515, 2021 https://doi.org/10.1038/s41598-021-81027-8

78. Pagtalunan ME, Miller PL, Jumping-Eagle S, Nelson RG, Myers BD, Rennke HG, Coplon NS, Sun L, Meyer TW: Podocyte loss and progressive glomerular injury in type II diabetes. *J Clin Invest* 99: 342–348, 1997 https://doi.org/10.1172/JCI119163

79. Yilmaz MI, Siriopol D, Saglam M, Kurt YG, Unal HU, Eyileten T, Gok M, Cetinkaya H, Oguz Y, Sari S, Vural A, Mititiuc I, Covic A, Kanbay M: Plasma endocan levels associate with inflammation, vascular abnormalities, cardiovascular events, and survival in chronic kidney disease. *Kidney Int* 86: 1213–1220, 2014 https://doi.org/10.1038/ki.2014.227

80. Gunay M, Mertoglu C: Increase of endocan, a new marker for inflammation and endothelial dysfunction, in acute kidney injury. *North Clin Istanb* 6: 124–128, 2018 https://doi.org/10.14744/nci.2018.70446

81. Honore PM, De Bels D, Attou R, Redant S, Gallerani A, Kashani K: Endocan removal during continuous renal replacement therapy: Does it affect the reliability of this biomarker? *Crit Care* 23: 184, 2019 https://doi.org/10.1186/s13054-019-2469-7

82. Su YH, Shu KH, Hu CP, Cheng CH, Wu MJ, Yu TM, Chuang YW, Huang ST, Chen CH: Serum Endocan correlated with stage of chronic kidney disease and deterioration in renal transplant recipients. *Transplant Proc* 46: 323–327, 2014 https://doi.org/10.1016/j.transproceed.2013.10.057

83. Çelik M, Sökmen E, Sivri S, Erer M: Reply: New insight into the cardiovascular prognostic importance of endocan. *Angiology* 70: 671, 2019 https://doi.org/10.1177/0003319719845961

84. Çağlar Torun A, Tütüncü Ş: Assessing the therapeutic effect of resveratrol in heart failure following blunt chest trauma and the potential role of endocan as a biomarker of inflammation using rats. *Ulus Travma Acil Cerrahi Derg* 25: 343–349, 2019 https://doi.org/10.5505/tjtes.2018.77246

85. Kosir G, Jug B, Novakovic M, Mijovski MB, Ksela J: Endocan is an independent predictor of heart failure-related mortality and hospitalizations in patients with chronic stable heart failure. *Dis Markers* 2019: 9134096, 2019 https://doi.org/10.1155/2019/9134096

86. Balta S, Mikhailidis DP, Demirkol S, Ozturk C, Kurtoglu E, Demir M, Celik T, Turker T, Iyisoy A: Endocan–a novel inflammatory indicator in newly diagnosed patients with hypertension: A pilot study. *Angiology* 65: 773–777, 2014 https://doi.org/10.1177/0003319713513492

87. Calderaro J, Meunier L, Nguyen CT, Boubaya M, Caruso S, Luciani A, Amaddeo G, Regnault H, Nault JC, Cohen J, Oberti F, Michalak S, Bouattour M, Vilgrain V, Pageaux GP, Ramos J, Barget N, Guiu B, Paradis V, Aubé C, Laurent A, Pawlotsky JM, Ganne-Carrié N, Zucman-Rossi J, Seror O, Ziol M: ESM1 as a marker of macrotrabecular-massive hepatocellular carcinoma. *Clin Cancer Res* 25: 5859–5865, 2019 https://doi.org/10.1158/1078-0432.CCR-19-0859

88. Kim JH, Park MY, Kim CN, Kim KH, Kang HB, Kim KD, Kim JW: Expression of endothelial cell-specific molecule-1 regulated by hypoxia inducible factor-1α in human colon carcinoma: Impact of ESM-1 on prognosis and its correlation with clinicopathological features. *Oncol Rep* 28: 1701–1708, 2012 https://doi.org/10.3892/or.2012.2012

89. Ozaki K, Toshikuni N, George J, Minato T, Matsue Y, Arisawa T, Tsutsumi M: Serum endocan as a novel prognostic biomarker in patients with hepatocellular carcinoma. *J Cancer* 5: 221–230, 2014 https://doi.org/10.7150/jca.7691

90. Yu PH, Chou SF, Chen CL, Hung H, Lai CY, Yang PM, Jeng YM, Liaw SF, Kuo HH, Hsu HC, Chen JY, Wang WB: Upregulation of endocan by Epstein-Barr virus latent membrane protein 1 and its clinical significance in nasopharyngeal carcinoma. *PLoS One* 8: e82254, 2013 https://doi.org/10.1371/journal.pone.0082254

91. Sagara A, Igarashi K, Otsuka M, Kodama A, Yamashita M, Sugiura R, Karasawa T, Arakawa K, Narita M, Kuzumaki N, Narita M, Kato Y: Endocan as a prognostic biomarker of triple-negative breast cancer. *Breast Cancer Res Treat* 161: 269–278, 2017 https://doi.org/10.1007/s10549-016-4057-8

92. Ekiz-Bilir B, Bilir B, Aydın M, Soysal-Atile N: Evaluation of endocan and endoglin levels in chronic kidney disease due to diabetes mellitus. *Arch Med Sci* 15: 86–91, 2019 https://doi.org/10.5114/aoms.2018.79488

93. Cikrikcioglu MA, Erturk Z, Kilic E, Celik K, Ekinci I, Yasin Cetin AI, Ozkan T, Cetin G, Dae SA, Kazancioglu R, Erkoc R: Endocan and albuminuria in type 2 diabetes mellitus. *Ren Fail* 38: 1647–1653, 2016 https://doi.org/10.1080/0886022X.2016.1229966